Consistency-Checking 3D Geological Models

Marion N. Parquer[1], Eric A. de Kemp[1], Boyan Brodaric[1] and Michael, J. Hillier[1]

Correspondance: Eric A. de Kemp
eric.dekemp@canada.ca
orcid.org/0000-0003-0347-5792

[1]Geological Survey of Canada,
 Three-dimensional Earth Imaging and Modelling Lab
 601 Booth Street, Ottawa, Canada, K0E 1E9

Abstract

3D geological modelling algorithms can generate multiple models that fit various mathematical and geometrical constraints. The results, however, are often meaningless to geological experts if the models do not respect accepted geological principles. This is problematic given the expected use of the models for various downstream purposes, such as hazard risk assessment, flow characterization, reservoir estimation, natural storage, or mineral and energy exploration. Verification of the geological reasonableness of such models is therefore important: if implausible models can be identified and eliminated, it will save countless hours, computational and human resources, as well as minimize user problems.

To begin assessing geological reasonableness, we develop a framework for consistency-checking and test it with a proof-of-concept tool. The framework consists of a space of consistent and inconsistent geological situations that can be held between a pair of geological objects, and the tool assesses a model against the space to identify (in)consistent situations. Both the framework and tool are successfully applied to several case studies as a promising first step toward automated assessment of geological reasonableness.

Keywords – geological knowledge, geological consistency, 3D geological modelling, temporal relation, spatial relation, polarity

1 Introduction

Geomodelling techniques are often deployed to bridge the spatial gaps between explored areas, including gaps in stratigraphic structure, property distribution, and target extent. Increased data availability and rising societal need for natural resources have recently stimulated development of advanced geomodelling modelling techniques such as stochastic simulation (Lajevardi and Deutsch, 2015), time-varying modelling (Hinojosa, 1993), Bayesian techniques (de la Varga and Wellmann, 2016), and direct perturbation of models or data (Lindsay et al., 2012). Wrapped into growing complex workflows (de Kemp et al., 2016), these new techniques can operate with scarce and heterogeneous data, are frequently deployed to model less accessible and more complex terrains, and often produce a wide range of equiprobable models and associated uncertainties (Wellmann and Caumon, 2018).

1

2 However, several problems can arise from these advanced techniques. For example, accuracy issues associated with

3 scarce data can become magnified and lead to geologically questionable spatial interpolations, such as older

4 geological units deposited on younger units (Figure 1). These issues might be further compounded by biases at each

5 modelling step or decreases in the reliability of the data as the number of participants increases (Bond, 2015). Data

6 may also become irrelevant due to scale discrepancies (Snyder et al., 2014), and degraded due to re-sampling to

7 meet coarser scale requirements or to suit algorithms that imprecisely fit data (Hillier et al., 2021). As data scarcity

8 and loss necessarily impact the accuracy and credibility of any model, multiple equiprobable realizations are often

9 generated in the hope that some model, or the mean of models, comes closer to representing reality and minimizing

10 uncertainty. Equiprobable models, though, are not necessarily geologically possible (Deutsch, 2018). Indeed, some

11 of the more data-driven 3D modelling methods can generate results that respect the data, but do not necessarily

12 respect established geological principles (Lyell, (1833) 2022). Conversely, purely knowledge-driven 3D modelling

13 methods might respect geological principles or 'norms' but might not fit the underlying data (Bai et al., 2017). Thus,

14 amongst a multitude of equiprobable models, it is unavoidable that a non-negligible number of them might produce

15 geologically unreasonable results. This is especially a challenge for hypothesis testing in natural systems, or

16 developing AI training sets, which might involve billions of such models.

17

18 The number of possible models therefore must be reduced, and this reduction can be accomplished in two ways: (1)

19 by building fewer and better models, or (2) by excluding inappropriate models. The first solution involves having

20 more and better data and knowledge, or improved algorithms. Increasing the amount of data in study areas, possibly

21 from diverse sources such as geophysical or structural data (Giraud et al., 2020, 2024; Wellman and Caumon, 2019;

22 Hillier et al., 2014; Grose et al., 2019; de la Varga et al., 2019), or improving data quality, increases overall accuracy

23 and reduces the number of possible models. Such results also might be achieved from increased constraints,

24 including refinements of knowledge such as input stratigraphy or augmentation of algorithms with implicit and rule-

25 based modelling (Bertoncello et al., 2013; Bai et al., 2017). Problematically, however, these solutions likely require

26 the acquisition of new data or knowledge, which is often impossible. It also might require the development of more

27 robust algorithms to improve model quality (Jessell et al., 2010; Cherpeau et al., 2010; Ranalli, 1980), such as

28 physics-based modelling approaches (Shokouhi et al, 2021; Hobbs et al. 2021), which are not yet mature.

1
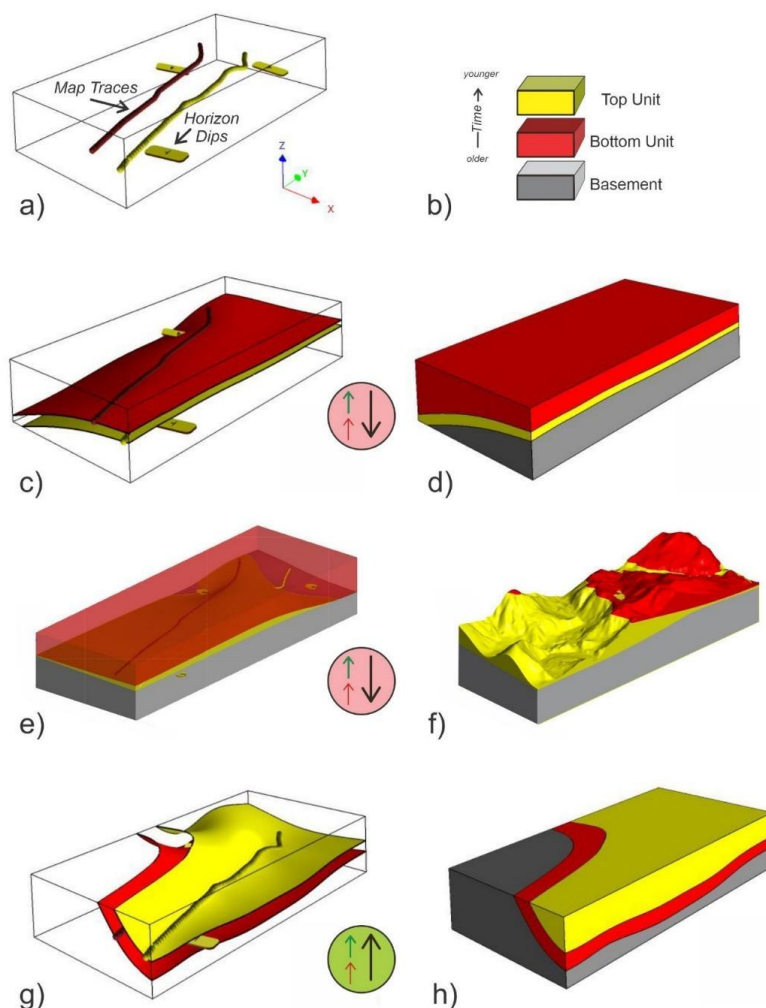
Figure 1. Example of *unreasonable* 3D geological models (c) to (f). Sparse input data (a) includes two separate depositional horizon traces and 3 gently dipping bedding constraints (yellow tablets) indicating depositional tops upward. The event history (b) has an older unit (red) deposited below the younger unit (yellow). However, use of the Lajaunie (1997) implicit method in SURFE (Hillier et al. 2014, 2021) results in the older unit deposited over the younger unit (c)-(d), which is unreasonable in the absence of other events. Similarly, using commercial software from LeapFrog Geo (Seequent), in (e) without topography and in (f) with topography, also indicates an unreasonable geological sequence with the older unit on top. In contrast, (g) and (h) show reasonable models generated with SURFE software tuned to respect a minimal horizon thickness and depositional history. Circled arrows show a deposition polarity vector for the older unit (red arrow), younger unit (green arrow), and the temporal direction (black arrow, from older to younger unit), as well as the geological plausibility of the situation: a green background indicates consistency with geological principles (aligned vectors), and the red background denotes an inconsistent scenario (unaligned vectors).

1   The second solution, which involves model exclusion, can be accomplished manually or automatically: (i) manually,

2   by having a geologist inspect and reject models using accumulated expertise; or (ii) automatically, by performing a

3   rapid computer-driven check to eliminate poor instances, during or after model construction. A significant

4   disadvantage of the manual approach is lack of reproducibility: as implicit knowledge can vary between and within

5   geologists (Brodaric *et al.*, 2004; Brodaric 2012, Bond 2015), it is unlikely manual corrections would be

6   reproducible for more than a few models, and the selection of a certain model would likely be unexplainable. In

7   contrast, if knowledge is made explicit (Brodaric and Gahegan, 2006), automatic approaches could be reproducible

8   and explainable, as per the consistency-checking approach in this paper. A critical aspect of this approach therefore

9   is the explicit digital encoding of knowledge, as well as its integration into geo-modelling workflows. Although

10   integration techniques like rule-based geomodelling (Pyrcz et al., 2015) and implicit modelling (Jessell et al., 2014)

11   are quite common, they typically incorporate a limited range of knowledge. Extending this range also is not new,

12   e.g. early work focuses on capturing knowledge from a geological map, cross-section, or other field record (Harrap,

13   2001; Burns, 1975; Burns and Remfry, 1976; Burns et al., 1978; 1969), but only recently have we begun such

14   extension for 3D geo-modelling (e.g., Jessell et al., 2021; Rauch, et al., 2019). In addition to limitations in

15   knowledge range, there exist accompanying limitations in its use, as the knowledge is utilized primarily *a priori* for

16   model-building rather than *a posteriori* for model evaluation. Key goals for a consistency checker then include an

17   expansion of the range of knowledge plus its effective application for consistency evaluation.

18

19   A first step to such expansion and evaluation might be the utilization of all information from a geologist's

20   observation sheet. However, it is very unusual to incorporate all such knowledge in a 3D model: much of it remains

21   reported on a map, e.g. as colours, abbreviations or symbols, and the rest in the map legend, in related articles and

22   reports, or in the mind of the geologist. In particular, the geological legend as we know can be incomplete (Harrap,

23   2001) and does not always contain the entire stratigraphic and structural history, prompting the development of a

24   'legend language' as a first attempt to formalize geological map knowledge for the purpose of checking the

25   consistency of traditional 2D geological maps (Harrap, 2001).

26

27   More recently, the topological aspects of geological maps and models have received significant attention as a

28   pertinent knowledge representation (Thiele et al., 2016a, b; Le et al., 2013). This includes the spatial relations

29   between discrete elements of a 3D model, particularly those unchanging under continuous deformation (Crossley,

1   2005), such as adjacency, inclusion or intersection. An important aspect is the dimensionality of the spatial objects,

2   which might be 0D (a point), 1D (a line), 2D (a surface), or 3D (a volume). Spatial relations between such objects

3   have been widely examined, with distinct relationships identified between 2D regions (Egenhofer and Franzosa,

4   1991) as well as 0D, 1D, 2D, and 3D regions (Zlatanova et al., 2004). They also have been applied to certain types

5   of geological objects (Schetselaar and de Kemp, 2006), providing a basis for the spatial component of geological

6   knowledge, and underpin efforts in knowledge-driven 3D geological model construction (Zhan et al., 2022; 2019).

7   However, they are not yet applied to the evaluation of geological models, especially in combination with temporal

8   relations, despite being applied to the evaluation of models in other domains (e.g. Van Oosterom, 1997; Gong and

9   Mu, 2000; Arora et al., 2021; Nikoohemat et al., 2021; Bezhanishvili et al. 2022).

10

11   In this paper we develop a knowledge framework and proof-of-concept tool for automated consistency-checking of

12   3D geological models. The knowledge framework consists of a space of (in)consistent geological situations holding

13   between nine kinds of geological objects, with each situation being a unique combination of a spatial, temporal and

14   polarity relation. The proof-of-concept tool then assesses the relations in a geo-model against the space to identify

15   (in)consistencies and is successfully applied to several case studies. The framework is presented in Section 2, the

16   tool is described in Section 3, several case studies are outlined in Section 4, some additional thoughts on the

17   consistency checker and geological reasonableness are presented in Section 5, and the paper concludes with a brief

18   recap in section 6.

19
20   **2 Geological Consistency-Checking Framework**

21   Geological knowledge is the accumulation of results from thousands of years of human inquiry into our natural

22   environment, with modern formal geological knowledge emerging in the mid 1800's (Lyell, (1833) 2022; Rothery,

23   2016). Such knowledge is found in digitally archived articles and books (e.g. Kardel and Maquet, 2012) as well as

24   online products and courses (e.g. Fattah, 2018). It is particularly useful to help understand the often hidden and

25   unobserved subsurface of the Earth. However, the various possible sources of data (e.g. surface mapping, boreholes,

26   geophysical surveys) generally cannot provide sufficiently uniform and continuous information for a volume of

27   interest. Supplementary geological knowledge is required for improved interpretation between sometimes extremely

28   sparse observations (Groshong, 2006; Frodeman, 1995), especially when coupled with new data integration

29   techniques and approaches (Giraud et al. 2020; Wellmann and Caumon, 2018).

1

2 For consistency-checking purposes herein, we distinguish between data and knowledge, with data being

3 observational and geological knowledge being either local or universal. Data then includes any form of observation

4 used to understand a specific geological area, e.g. bedding top indicators, structural orientations, fault and horizon

5 contacts or seismic picks, or geophysical readings. Local knowledge applies to a specific area but is not

6 observational: it is interpretational and includes things such as the local stratigraphy and process history. In contrast,

7 universal geological knowledge, or 'norms', apply to different geographical areas and includes things such as

8 general laws, principles, process types, and classification systems, e.g., Walther's Law, uniformitarianism, the

9 notion of deposition, rock type classification. Significantly, data and knowledge are interconnected insofar as

10 knowledge is inferred from data, and the data is contextualized by knowledge during observation and interpretation

11 (Brodaric et al, 2004). Indeed, both data and knowledge are required to arrive at any interpretation, including a 3D

12 geo-model. Consistency then can be seen as the degree of agreement between a model and the relevant data and

13 knowledge. However, current modelling techniques are primarily focused on ensuring and assessing data

14 consistency, with knowledge consistency less developed, e.g. implicit modeling techniques typically optimize fit to

15 data and assume stratigraphic consistency, but such consistency might not be achieved by all techniques (see Figure

16 1), and further might not be reflected in all geometric realizations due to idiosyncrasies of spatialization algorithms

17 (Hillier et al., 2021).

18

19 Therefore, some geological models can still fail to respect basic geological norms. To determine knowledge

20 consistency for a 3D geo-model, we expect local knowledge to be typically derived from a 2D map legend, cross

21 section, or associated report, whereas universal knowledge is preexistent, in our case as core types of geological

22 objects, foundational spatial, temporal and polarity relations. Truth Tables then denote all possible combinations of

23 these relations for pairs of object types, with each combination being a situation identified as consistent or

24 inconsistent. Knowledge consistency is finally assessed by traversing the spatial relations between pairs of objects in

25 a geo-model, using the local knowledge to determine object types, temporal relations, and polarities of the objects,

26 which together form an index into the Truth Tables to determine the (in)consistency of a specific situation.

27

28

29

2.1 Geological Objects and Polarity

The objects in a 3D geo-model (geo-objects) are, for the purposes of this paper, representations of instances of nine

distinct geological object types: depositional unit, intrusion unit, extrusion unit, metamorphic unit, fault, erosion

surface, fold volume, and linear and planar fabric. Note that horizons, understood as the top or bottom surfaces of a

volume, are excluded from the list of geological objects primarily because, in effect, they imply a volume and are

thus already included. This does not exclude the top or bottom surfaces of volumetric entities from being

represented in 3D geo-models, but they are not distinct geological object types in this paper and are converted to 3D

volumes for consistency-checking in our proof-of-concept tool. Additionally, we utilize two types of polarity

associated with geological objects. The first type of polarity is an internal vector pointing in the direction of creation

or destruction of an object's material: e.g. for depositional units, from the base or oldest part of the geological body

to the top, in the direction of material creation; and for erosional surfaces from the top to bottom of the eroded rock

body, in the direction of material destruction. Volumetric geo-objects are assigned a gross internal polarity valid for

the object as a whole, but some immaterial objects, of lower-dimensionality, lack polarity as they are not associated

with material growth or destruction, e.g. fault surfaces. Those with a gross internal polarity might also have many

local polarities distributed throughout the object, constituting in sum a polarity field for the object and forming a

basis for determining its gross polarity. The second type of gross polarity is an age direction vector shared by two

geo-objects, pointing from the older to the younger object and set parallel to one of the internal polarities of the

objects. Thus, collectively, there possibly exist three gross polarity vectors associated with a pair of geo-objects: the

growth direction vector within each object, and the age direction vector across the objects. The alignment of these

vectors then helps determine the geological plausibility of the situation (see Figure 1). The nine types of geo-objects,

and associated polarities, include:

- Depositional unit: a rock volume primarily generated by gravitational, water or air mediated, material
  accumulation processes, and associated with a time interval. The gross internal polarity is unidirectional
  and perpendicular to the upper depositional surface (Figure 2a): for a given sedimentary unit, it points up in
  the opposite direction of gravity at the moment of deposition.

- Extrusion unit: a rock volume primarily generated by igneous extrusive processes and associated with a
  time interval. The local internal polarities typically point radially upwards to a proximal vent or feeder
  facies. This includes internal polarities associated with deposition of eruptive material, which is affected by
  gravity and tends to flow downhill, but with airfall material accumulating upward. A gross internal polarity

vector thus points upwards at the time of formation, similar to sedimentary units. However, extrusive units with variable growth directions in subglacial situations are an exception, having chaotic eruptive depositional internal polarity vectors that cannot be characterized by a single gross vector.

- Intrusion unit: a rock volume primarily generated by igneous subterranean processes and associated with a time interval. Its internal polarities radiate from a core region towards the cooling host rock contact surfaces (Figure 2c), with a gross internal polarity set to a representative direction. Many configurations for the growth gradients in these bodies exist, but in general the emplacement contacts with host rocks are similar to unconformities, in that they tend to be truncating earlier material through magmatic erosion, assimilation or expansion (Annen, 2011).

- Metamorphic unit: a rock volume primarily generated by deep thermal-kinetic processes and associated with a time interval. The internal polarities are perpendicular to the metamorphic isograd and pointing to the lower metamorphic grade or into the host protolith (Figure 2d). However, in many cases a gross internal polarity vector can be set pointing upwards from a core heat source. This holds for a regional perspective, in which we can envision the earth's regional geothermal gradient as pointing from hotter-deeper to cooler-shallower lithospheric material. It also holds for a local perspective, in which the location of the source of metamorphism and hence the local gradient may be easier to establish from metamorphic aureoles around intrusions.

- Fault surface: a spatial (immaterial) surface between displaced rock volumes that were once continuous, and associated with a time instant or interval for the displacement activity (Figure 2e). The surface lacks internal polarity, as it is never constituted by any material. We are not, at this stage in our approach, considering polarities from kinematic properties distributed on faults such as slip displacement directions.

- Erosion surface: a spatial surface where a rock volume has completely eroded via a mechanical process. It is associated with a time interval or instant indicating the end of the erosion process. Its gross internal polarity points towards the eroded unit, in the direction of material destruction (Figure 2f); typically, this direction will be opposite to that of an overlying sedimentary unit.

- Fold volume: a rock volume affected by ductile tectonic deformation processes with an associated time interval. The fold volume can be composed of depositional, intrusive, extrusive, or metamorphic material, since these units can all become folded, as can an earlier fault or erosional surface. The gross internal polarity points in the direction of structural vergence or tectonic transport direction (Figure 2g). For our

1   purposes, nappes, duplex structures and orogenic scale tectonic units could be classified as fold volumes.

2   They may contain multiple folding events and have fold-fold relations. We do not treat these in this study

3   but consider they could be dealt with using a similar consistency approach. For example, an older fold set

4   cannot re-fold a younger generation of folds.

5   ● Linear fabric: A penetrative preferential linear orientation within a pre-existing rock material, with an

6   associated time interval. Some objects such as paleocurrents could have a unidirectional (Figure 2h) or

7   bidirectional gross internal polarity such as from tidal currents, but a fold hinge line has no preferred

8   direction (polarity).

9   ● Planar fabric: A penetrative preferential planar orientation within a pre-existing rock material, with an

10   associated time interval. A primary planar deposition fabric has a normal with a positive upward polarity at

11   the time of formation (Figure 2i), (i.e., bedding top observations). A metamorphic planar fabric has a

12   normal with no polarity unless it can be derived from its host metamorphic unit. Igneous fabrics may have

13   derived polarity direction based on crystal accumulation, igneous flow layering or emplacement contact

14   directions. All fabrics (linear and planar) will have spatial, temporal topological relations and possible

15   polarity properties, that could be considered in determining feature-to-feature relation validity.

16

17   Field geologists typically infer these geo-objects and associated geological histories by interpreting common spatial

18   and temporal patterns across field sites. These patterns involve geological relations held between geological objects,

19   thus providing a simple topological framework for possibly complex geological situations. Major geological

20   relations, or situations, further can be decomposed into combinations of spatial, temporal, or polarity relations. For

21   example, if Sandstone-A is a depositional unit and Granite-B is an intrusion unit, and Sandstone-A is *intruded-by*

22   Granite-B, then we also expect a spatial relation such as Sandstone-A *spatially meets* Granite-B, a temporal relation

23   such as Sandstone-A *is temporally met by* Granite-B, and the gross internal polarities are either *aligned* or *opposed*.

24   In this way, the *intruded-by* relation might be decomposed into a specific combination of a spatial, temporal, and

25   polarity relation. The task of a consistency checker then can be seen as verifying the validity of such a relation

26   combination/situation.
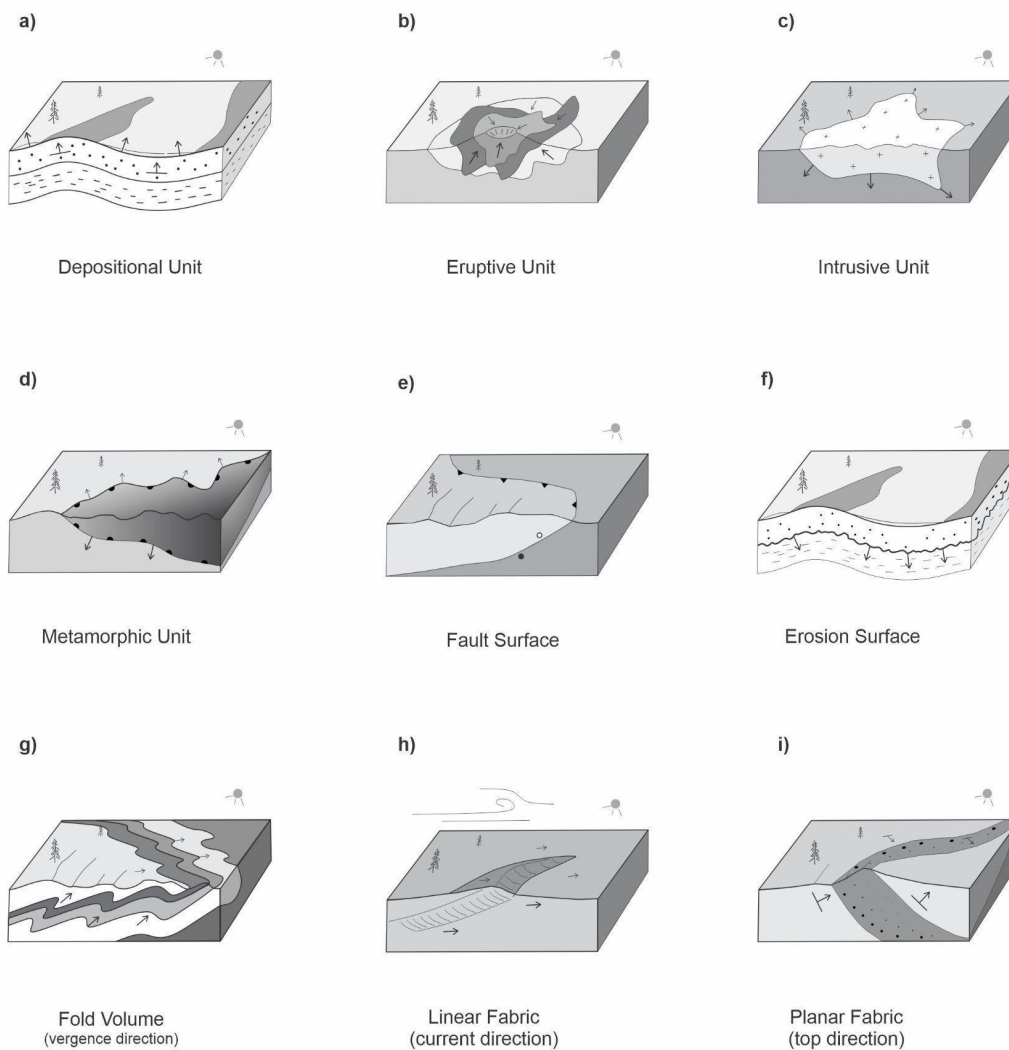
Figure 2. Examples of geological objects with polarities, symbolized with black arrows. Note there is no polarity for fault features (e).

1

2 **2.2 Spatial Relations**

3 Prominent formalisms for binary spatial relations are derived from two main approaches (Galton 2009): Region

4 Connection Calculus (RCC) and the 9-intersection model (9I; Egenhofer, 1989; Egenhofer et al., 1993, Egenhofer

5 and Franzosa, 1991). In this paper we informally adapt the 9I approach, implemented for 0, 1, 2 or 3D objects and

6 512 possible spatial relations (Zlatanova et al., 2004). However, these 512 possibilities are drastically reduced for

7 typical geological situations in 2D and 3D (Schetselaar and de Kemp, 2006), resulting in 40 spatial relations for the

8 nine geological object types, as shown in Figure 2; then for any pair of spatial objects only one spatial relation can

9 hold. These relations can be represented as a three-part tuple, as shown in Tuple Equation 1. The tuple is also

10 directed or not, depending on the symmetry of the relation, given that asymmetric relations are directional and

11 symmetric relations are not directional; e.g. *meets* is symmetric, so if A *meets* B then B meets A, thus *meets* is not

12 directional; but if A *contains* B then it cannot be the case that B *contains* A (or A *is contained by* B), so *contains* is

13 asymmetric and directional. The symmetric spatial relations from Table 1 are *is disjoint with*, *meets*, *overlaps*,

14 *equals*, *intersects*, and the remaining relations are asymmetric. Symmetric relations also are their own converse,

15 whereas asymmetric relations have distinct converses, such as A *contains* B and B *is contained by* A.

16

17
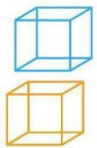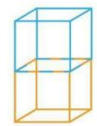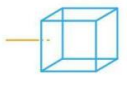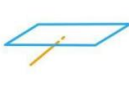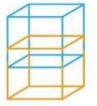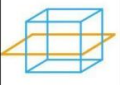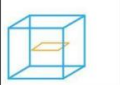
$$
Entity_A
\begin{Bmatrix}
isdisjointwith \\
meets \\
overlaps \\
contains \\
iscontainedby \\
covers \\
iscoveredby \\
equals \\
intersects
\end{Bmatrix}
Entity_B
\qquad (1)
$$

18

19

Spatial Relations	3D/3D	3D/2D	3D/1D	2D/2D	2D/1D	1D/1D
A is disjoint with B						
A meets B						
A overlaps B						
A contains B						
A is contained by B						
A covers B						
A is covered by B						
A equals B						
A intersects B						

1

2

3 **Table 1.** The 9 spatial relations between two geological objects of 1/2/3 dimensions. Blank gray cells denote
4   impossible spatial relations after Egenhofer (1989); Egenhofer et al. (1993); Egenhofer and Franzosa (1991);
5   and Zlatanova et al. (2004).
6

7

8

9

1 **2.3 Temporal Relations**

2

3 Temporal relations are required to establish a temporal ordering between geological objects (Perrin et al., 2011).

4 Though the temporal position of a geological object is not always known (Michalak, 2005), the temporal ordering

5 between objects can be derived from the timeline of associated generative events (Galton, 2009; Claramunt and

6 Jiang, 2001). As with spatial relations, dimensionality plays a role: temporal relations can be categorized according

7 to the nature of the time duration (of the event) with 3 potential combinations: period/period, period/instant, or

8 instant/instant. Building on Allen's definitions (Allen, 1983), this leads to 14 distinct temporal relations, including

9 converses (e.g. A *precedes* B and B *is preceded by* A), as shown in Table 2, for the nine geological object types;

10 moreover, for any pair of objects only one temporal relation can hold. Of note is the *is incomparable to* relation,

11 which indicates the temporal ordering is unknown due to unavailable temporal knowledge about one or both objects.

12 Tuple Equation 2 illustrates the three-part tuple for expressing these relations. The symmetric relations are *equals*

13 and *is incomparable to*, with the remainder being asymmetric.

14

15

$$Entity_A \begin{cases} precedes \\ meets \\ overlaps \\ isfinishedby \\ contains \\ starts \\ equals \\ isincomparableto \\ isstartedby \\ isduring \\ finishes \\ isoverlappedby \\ ismetby \\ isprecededby \end{cases} Entity_B \qquad (2)$$
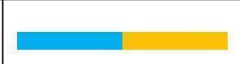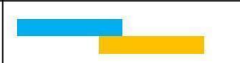
16
17
18

19

temporal relations	period / period	period / instant	instant / instant
A precedes B *B is preceded by A*			
A meets B *B is met by A*			
A overlaps B *B is overlapped by A*			
A starts B *B is started by A*			
A finishes B *B is finished by A*			
A during B *B contains A*			
A equals B			
A is incomparable to B			

Table 2. The 14 temporal relations between two geological objects, after Allen (1983). The temporal timeline advances from left to right in each cell. Blank gray cells denote impossible temporal relations, and blank white cells denote unknown temporal relations.

2.4 Polarity Relations

A polarity relation can be determined from up to three independent component polarities (discussed earlier in Section 2.1); the two internal polarities, dependent on the type of geo-object and processes governing its formation, and the age polarity. The internal and age polarity vectors, can be compared to determine if they are 'aligned' or 'opposed', such that:

- Aligned polarity relation: the vectors are roughly parallel, such that each vector is within 90° of every other vector.
- Opposed polarity relation: a vector is oriented in an opposite direction to the others, such that one vector is at least greater than 90° from one of the others.

If an object does not have internal polarity, such as a fault, or the internal polarity is missing due to lack of knowledge, then the polarity relation defaults to aligned. Importantly, polarity alignment or opposition does not

1   necessarily determine (in)consistency alone, as such determination requires consideration of the spatial and temporal

2   relations. For example, opposed internal polarity can indicate either inconsistency or consistency: e.g. touching

3   depositional units with opposed internal or temporal polarities are inconsistent (Figure 3b), because such units must

4   create material in the same spatial and temporal direction; but a touching depositional unit and erosional surface

5   with opposed internal polarity are consistent, because the surface must erode material towards the older unit (Figure

6   3e). The internal polarity relation also might not play a determining role in assessing (in)consistency, as the spatial

7   and temporal relations may individually or together be determining factors: e.g. the (in)consistency of an intrusion

8   into a host depositional unit can be determined without regard to internal polarities (Figure 3c-d), as the intrusion

9   must be younger and touching the unit, otherwise some interceding object such as a fault or erosional surface is

10   missing from the model; similarly for a depositional unit and a fault surface (Figure 3g-h), as the unit must pre-exist

11   the fault. Note we do not consider growth faults to be strictly synchronous within a full unit, since at least some of

12   the material needs to pre-exist the faulting. On the other hand, there may not be any age polarity information

13   available other than what can be derived from the internal process vector directions. In the case of intrusions this can

14   be observed from cooling margins, inclusions along contacts and other textures indicating internal growth and

15   assimilation direction. Also note cases needing all three polarity components might be unaligned if the age polarity

16   is unaligned with either of the internal polarities (see Figure 1,c-f). A general framework for (in)consistency

17   therefore must consider the spatial, temporal, and polarity relations. This is accomplished by using these relations as

18   an index into 'Truth Tables' representing geological norms and specifying the (in)consistency of the situation (see

19   Section 2.5).

20
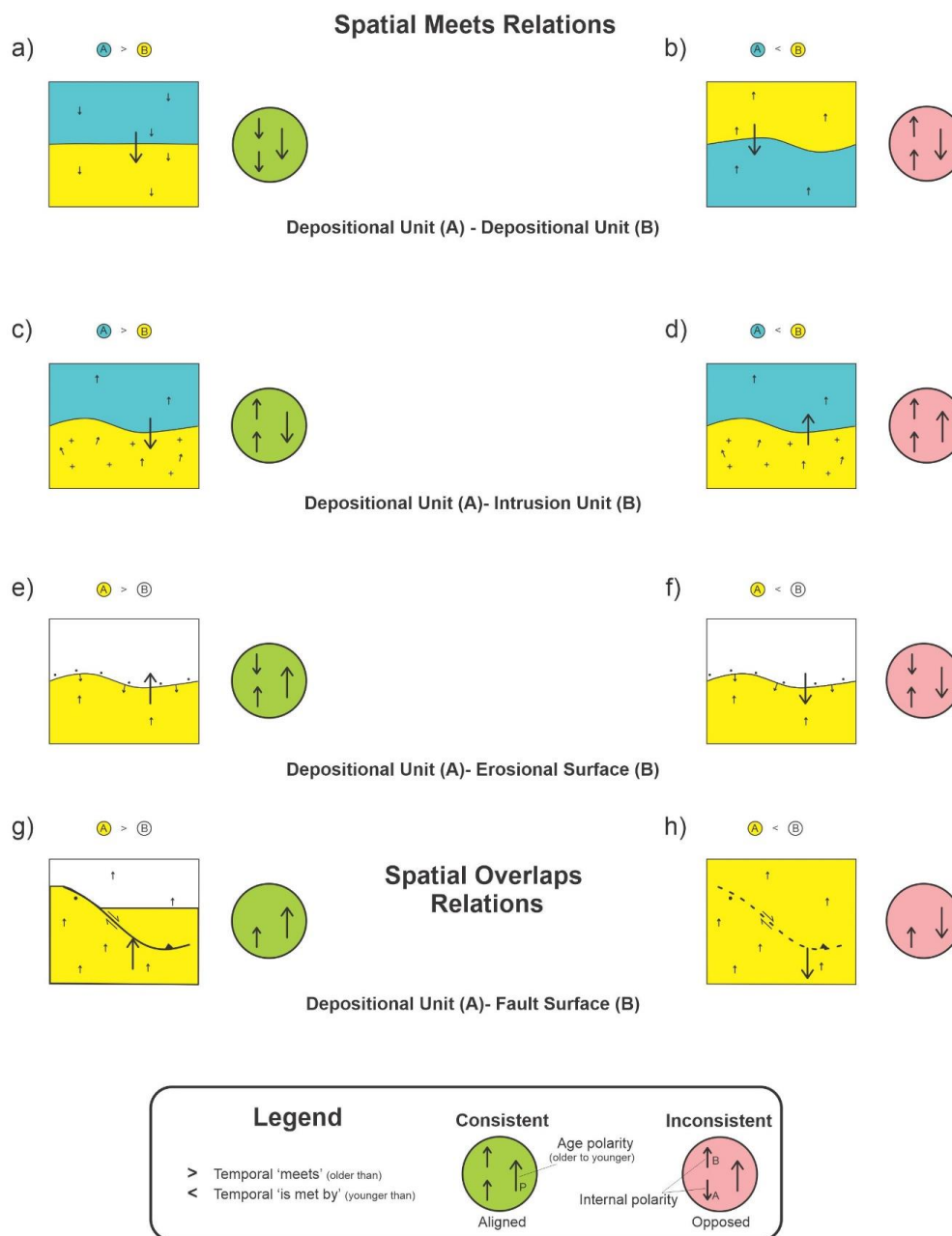
Figure 3. Examples of consistent (green circle) and inconsistent (red circle) polarity configurations for the spatial meets and overlaps relations; included are two vectors for internal polarity (small arrows) and a third age polarity vector pointing to the younger object (large arrow). A consistent scenario between two depositional units is depicted in (a), allowing overturning since overturning happened AFTER the binary relation has been established. An inconsistent scenario between such units is depicted in (b), as the age polarity is opposed to

both internal polarities, implying a third event between the unreasonable deposition of older on younger material. In (c) the deposition - intrusion unit scenario is consistent, as the age vector is aligned with the intrusive process, whereas in (d) it is not allowed because the host depositional unit is younger than the intrusion unit. In both (c) and (d) the internal polarities do not impact consistency evaluation, as age is the determining factor. In (e) and (f) the erosional surface needs a pre-existing material to erode, thus the direction of material reduction of the eroding surface moves into the older underlying depositional material. For a consistent scenario the age vector points from older unit to younger erosional surface (e), and for an inconsistent scenario, the age vector points from the younger surface to older unit (f). In (g) the fault has no internal polarity but needs a material object to displace. When the depositional unit pre-exists, as in (g), the relation is valid; however, in (h) the depositional unit is younger and did not exist when the fault evolved, so the relation is inconsistent.

2.5 Truth Tables

Many geological principles, known implicitly to geologists, must be considered in assessing, even grossly, the

consistency of the spatial, temporal, and polarity relations between two geological objects. Amongst the foremost

are stratigraphic considerations (Ziggelaar, 2009; Aubry et al., 1999):

- principle of lateral continuity: in general, a given object has the same age over its full extent.
- principle of actualism: past objects are formed by processes (tectonism, magmatism, deposition …)
  acting in the same way as today.
- principle of paleontological identity: two objects with the same fossils are considered contemporary.
- principle of superposition: without structural disruption events, a given object is younger than the
  object it covers and older than the one covering it.
- principle of horizontality: sedimentary objects deposit in nearly horizontal orientation; in general, a
  non-horizontal sedimentary sequence is generally deformed after its deposition.
- principle of cross-cutting: a given material layer is older than objects cross-cutting it.
- principle of inclusion: an object included into another object is older than the including object, except
  when a younger object internally displaces the enclosing object (i.e. dyke, sill, migmatite melt phase).

For the nine types of geological objects considered herein, 45 valid pairwise combinations of objects are identified

that respect these principles: $45 = (2 + 9 - 1)! / 2! (9 - 1)!$. For each object combination, a ternary "Truth Table"

establishes all possible consistent and inconsistent spatial-temporal-polarity relations: spatial relations along one

side, temporal relations along another side, and internal polarities along a third side; each table cell then can be

marked as consistent or inconsistent for the pair of objects. Although the 45 tables exist in draft form, for the

1   purposes of this paper we concentrate on the 7 tables relevant to the case studies (see the supplementary data

2   provided at de Kemp, 2024).

3

4   **Table 3.** Truth Table showing consistent (green) and inconsistent (red) spatial-temporal-polarity relations between
5   two depositional units. All 14 temporal relations are not included (as columns), for reasons of space and
6   because the values are duplicated for the inverse temporal relations.

7

8   The Truth Table in Table 3 illustrates all possible spatial-temporal-polarity relation combinations for two

9   depositional units. The eight columns represent the temporal relations possible between two intervals of time; the

10   remaining inverse temporal relations are excluded for reasons of space and redundancy, as the values in each row

11   are repeated for the temporal inverse, e.g. A *precedes* B and A *is preceded by* B are both red (inconsistent). The

12   rows represent the possible spatial and internal polarity relations between two depositional rock volumes. Green

1   cells then indicate consistent combinations, red cells inconsistent combinations, with the consistent cells being far

2   less numerous. Indeed, in Table 3, two distinct depositional units can be spatially related only via *is disjoint with* or

3   *meets*, once material sharing is excluded. All combinations are possible for spatially disjoint units, but only aligned

4   polarity is valid for units that spatially meet, because opposed polarities would signal inconsistencies, such as

5   missing events or intermediary objects.

6

7   In addition to the general geological principles, the following criteria are applied to the truth tables:

8   ●   Order and type of relata: the type of each relatum is fixed across all relations in a Truth Table. For example,

9   for a Truth Table between a depositional unit A and intrusion unit B, A is the first relatum and B is the

10   second relatum for all relations in the table, e.g. A *meets* B, A *precedes* B, B *is preceded by* A, and A *is*

11   *aligned with* B. This ensures all possible relation combinations are considered for the pair of objects.

12   ●   Material sharing: only some, not all, geological objects can share material: depositional, intrusion,

13   extrusion, or metamorphic units cannot share material *at any time*, because they cannot simultaneously

14   occupy the same space. These units, however, can share material with a fold volume, since the fold acts to

15   geometrically transform other material volumes. Furthermore, although there exist many scenarios in which

16   geological objects share material, e.g. a depositional unit and its parts, such as group and its formations,

17   however for the purposes of this paper we exclude all such cases, mainly because 3D algorithms tend to

18   bulk together geological components into single packages, such as a series, or model them as facies. As a

19   result of this material-sharing limitation, the *overlaps*, *contains*, or *covers* relations, and their converses,

20   can only hold between certain volumetric geological objects.

21   ●   Spatial relations: the following are assumed: (1) geological objects can be spatially disjoint and possibly

22   very far apart, e.g. on different continents, allowing all temporal relations; (2) only geological objects in

23   their full-dimensional form are valid, e.g. volumes can't be represented as lower dimensional top or bottom

24   surfaces, or a fault surface by a line. Implementation of this approach to consistency-checking thus requires

25   the conversion of all lower-dimensional representations to their full-dimensional counterparts.

26   ●   Model completeness: 3D geo-models are assumed to be complete. Therefore, any two geological objects

27   that touch or share material cannot have objects missing between them, such as an intermediary erosional

28   surface or fault. Without this assumption, the range of consistent scenarios becomes extremely large, with

29   significantly fewer inconsistent scenarios, and the effectiveness of the approach diminishes. In contrast,

1   with this assumption, inconsistent scenarios can signal (but not identify) the absence of spatial

2   intermediaries, which is useful during model-building.

3

4   **3 Geological Consistency-Checking Tool**

5   The consistency checker workflow is presented in Figure 4. This workflow aims to detect the consistency of 3D geo-

6   models given knowledge inputs of:

7   ●   a 3D geo-model;

8   ●   local knowledge consisting of relative or absolute ages, internal polarities, types of geological objects, and

9   ●   universal knowledge in the form of geological norms (i.e. Truth Tables).

10   After traversal of the 3D geo-model, the consistency checker constructs three intermediary products:

11   ●   a geo-object list, itemizing the geometric objects with internal polarities in the geo-model;

12   ●   a matrix of temporal relations for each pair of geological objects;

13   ●   a matrix of spatial relations for each pair of geological objects;

14   Then, as per Algorithm 1 (see Appendix): for each pair of geologic objects, the checker obtains their spatial relation

15   from the spatial relation matrix, their temporal relation from the temporal matrix, and their internal polarity direction

16   from the internal polarity property of individual objects. These are all then used as a 3 component (spatial-temporal-

17   polarity) index into a cell within the appropriate geo-object pair Truth Table to determine consistency. Each geo-

18   object pair is navigated to identify any inconsistent regions, which if present are output as a list of inconsistencies in

19   the geo-model. The tool is written using the proprietary Geodes-Solutions spatial toolkit (Botella et al., 2016;

20   Geodes-Solutions; Pellerin 2017), which facilitated spatial navigation and enabled conversion to a full-geometric

21   spatial representation. It was run on a moderately powerful Windows desktop, typically requiring several seconds to

22   minutes to assess a model from the case studies. Note the tool is written strictly to demonstrate proof-of-concept for

23   the framework and its use, and is not meant for widespread deployment being restricted to a specific, older, version

24   of the toolkit and tuned to the specific case studies.

25
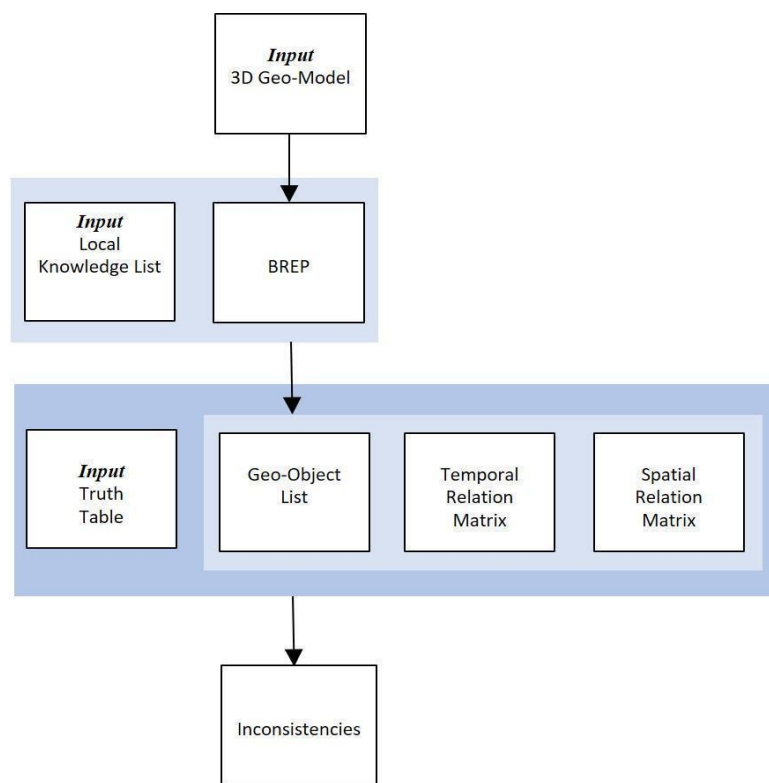
1

2 **Figure 4.** Consistency checker workflow.
3

4 **3.1 Local Knowledge List**

5 Local geological knowledge is specific to each study area and, alongside the 3D geo-model, is a primary input to the

6 consistency checker tool. It is found in a variety of sources external to the 3D geo-model, such as databases, map

7 legends, stratigraphic columns, journal articles and other reports. For the synthetic model shown in Figure 5a, a local

8 knowledge list is developed and illustrated in Figure 5b: the list contains the name of the geological object, its type

9 (from the nine possibilities), gross internal polarity and its relative age. For simplicity in the proof-of-concept tool,

10 an object's gross polarity is either up, down, or unknown. Furthermore, if a geological object is an aggregate of

11 parts, then the local knowledge applies to the aggregate and is assumed to be the same for every part. For example,

12 in Figure 5a, the local knowledge for units A and B is assumed to also hold for each of their parts A1, A2, B1, B2;

13 separate local knowledge for these parts, if it existed, would not be used. This enables the spatial, temporal, and

14 polarity to hold between the aggregates, which tends to be the resolution at which the input knowledge is available.

15

1
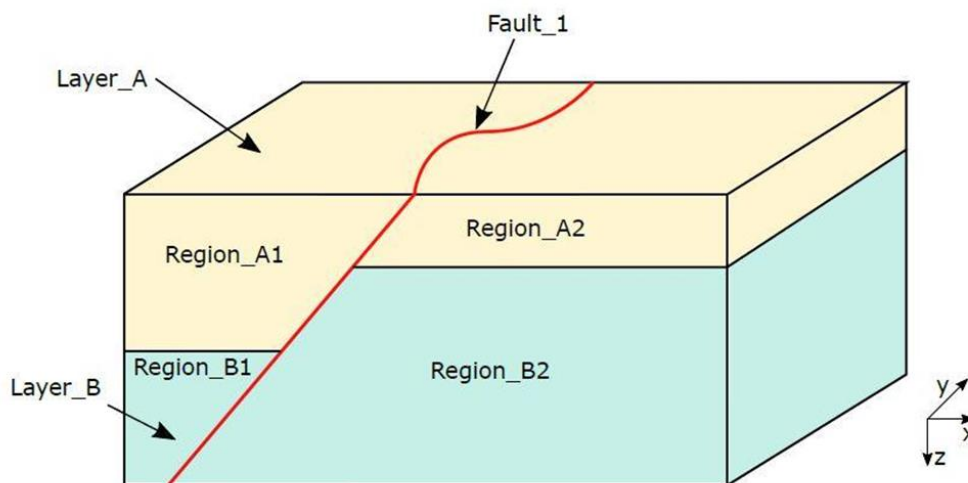
Figure 5a. example 3D geo-model.

3

4

Geological entity name	Geological entity type	Geological entity polarity	Geological entity age
layer_A	depositional unit / intrusion / extrusion / metamorphic unit / fault / erosion surface / fold volume / linear fabric / planar fabric	up / down / unknown	intermediate
layer_B	depositional unit / intrusion / extrusion / metamorphic unit / fault / erosion surface / fold volume / linear fabric / planar fabric	up / down / unknown	oldest
fault_1	depositional unit / intrusion / extrusion / metamorphic unit / fault / erosion surface / fold volume / linear fabric / planar fabric	up / down / unknown	youngest

5
6

Figure 5b. Local knowledge list for the model in Figure 5a.

8
3.1 Temporal Relation Matrix

Temporal relations are also obtained from external sources, including absolute or relative ages for each geological

object, as well as the kind of duration of the geological event (i.e. interval or instant). This knowledge then

determines the appropriate temporal relation between all pairs of geological objects, organized as a temporal matrix

(Figure 6). The matrix is developed manually for our case studies but could be determined automatically from

databases and other digital sources. The *incomparable* relation is chosen if there exists insufficient knowledge to

determine the temporal relation between a pair of objects.

Figure 6. Temporal relation matrix for the model in Figure 5a.

3.2 Spatial Relation Matrix

This matrix typically requires transformation of the 3D geo-model into a boundary representation (BREP; Banerjee et al., 1981), which ensures all geological objects are represented in their full-dimensional form, e.g. a volume initially represented by its top and bottom surfaces is converted into a mesh of the full exterior limits of the volume, consisting of faces, edges and vertices. A geo-model then can be traversed by following the geometric decomposition of each object and their adjacencies. If objects are named and typed (e.g. as in the Geodes-Solutions BREP solution; Botella et al., 2016; Geodes-Solutions; Pellerin 2017), then such traversal enables building of the spatial relation matrix. Specifically, the consistency checker builds a list containing each geometric object, as well their dimensionality (volume, surface, or line), type (e.g. depositional unit), and name (e.g. "Layer_A"). The list is traversed in order of dimensionality, starting with higher-dimensional objects (volumes) and progressing to lower-dimensional objects (surfaces and lines), with spatial relations determined between pairs of objects by inspecting decompositions and adjacencies. The results are recorded in the spatial relation matrix (Figure 7). For simplicity, a cell in the spatial matrix contains a single value, and the entities being related are the whole objects, e.g. Layer_A (Figure 5a), and not their fragments, e.g. Region_A1 or Region_A2 (Figure 5a). This is obviously problematic as fragments of objects might be spatially related in many ways, e.g. some might touch and others are disjoint, so the wholes can be related in many ways too, requiring multiple values per cell for each pair of wholes: e.g. it is possible Region_A1 has one relation with Region_B1 and a different relation with Region_B2, thus A would have multiple distinct relations with B. In such cases, the most dominant relation is selected, which suffices for our case studies.

1   To avoid multi-valued cells, a rigorous approach would utilize object fragments for consistency-checking, rather

2   than wholes. This issue and the incorporation of local relations is an important topic for future research.

3

4   **Figure 7.** Spatial relation matrix for the model in Figure 5a.
5

6   **4 Case studies**
7
8   The consistency checker is tested in four case studies: three synthetic models in which inconsistencies are

9   introduced, and a real regional geo-model from ongoing project work in Western Canada (Thapa and McMechan,

10   2019, McMechan et al., 2021). The geo-models are built using a variety of 3D modelling software and underlying

11   approaches including: Noddy (Jessell, 1981), GOCAD/SKUA (Jayr et al, 2008; Mallet, 2004), GOCAD (Mallet,

12   1989) and certain extensions, namely SURFE (Hillier, et al. 2014; de Kemp et al. 2017) and SPARSE (de Kemp et

13   al. 2004).

14

15   **4.1 Implicit Case study**

16   A simple but common modelling error occurs when applying certain implicit algorithms to sparse observations of

17   near parallel, shallow, dipping strata. Then, as depicted in Figure 1, if some older unit data are slightly

18   topographically higher than younger unit data, algorithm bias can result in older units above younger units. To

19   assess such a model, the consistency checker requires alignment of the three polarity vectors, two internal and one

20   temporal: as shown in Figure 8, the Truth Table indicates two depositional units that spatially and temporally meet

21   are (1) consistent, if the polarity vectors are aligned, and (2) inconsistent, if they are opposed. Therefore, this model

22   is evaluated as inconsistent, because the temporal polarity vector is opposed to the internal polarity vectors. Note

1   that there could be many reasons for the temporal reversal but this is not identified by the checker, e.g. it might be

2   algorithmic bias or missing objects, such as absent thrust faults, recumbent folds, or erosional surfaces.

3
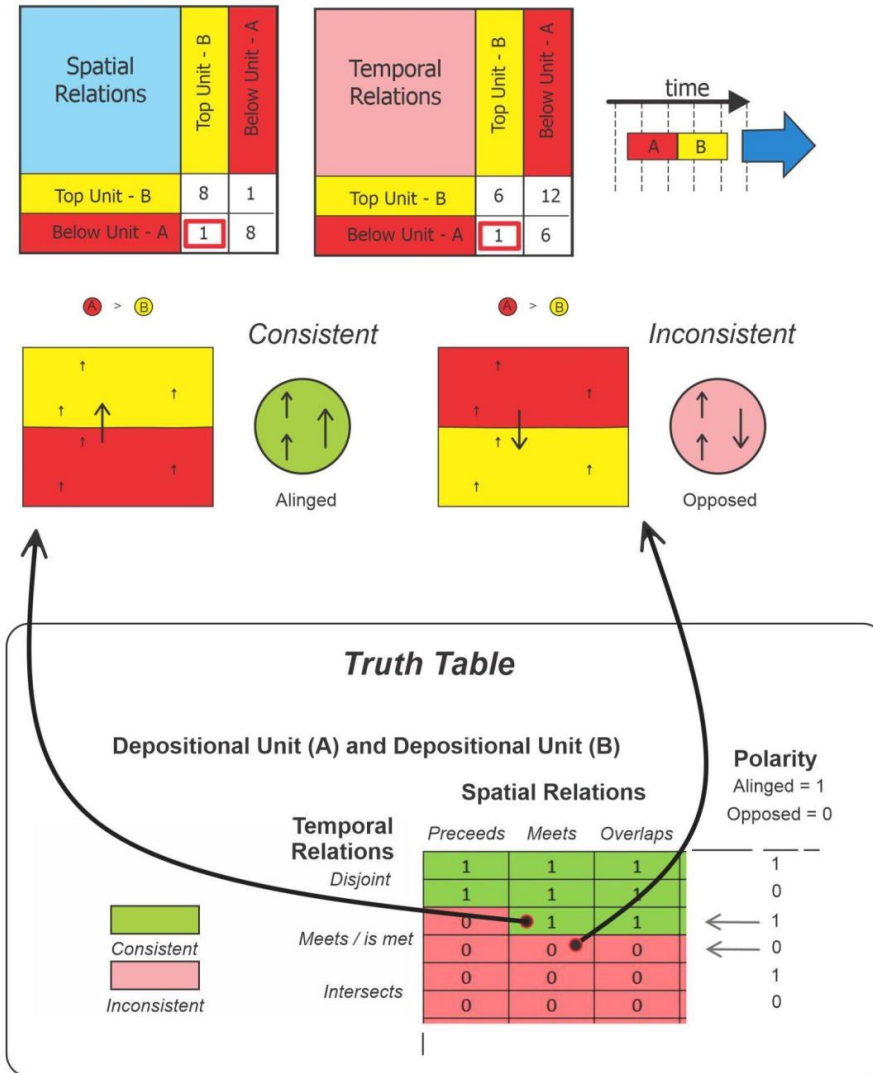
Figure 8. From the simple model in Figure 1, the internal polarity vectors are aligned with each other, but opposed
to the age vector. As the units both spatially and temporally meet, the Truth Table shows this configuration is
inconsistent due to the unaligned age vector.

1   **4.2 GOCAD/SKUA Case Study**

2   This synthetic model contains two depositional units, one intrusion, two faults, one fold, and one erosional feature

3   that is the top surface of the oldest unit (Figure 9). The model is created with GOCAD/SKUA (Mallet, 1989, 2004)

4   using the Structural and Stratigraphic workflow (Jayr et al., 2008); the local knowledge list (Table 4) and temporal

5   matrix (Figure 10) are developed artificially. The spatial matrix (Table 5) includes a variety of spatial relations, such

6   as touching geological units, faults cutting geological units, intrusion units protruding into other geological units, as

7   well as disjoint geological objects. As expected, results from the consistency checker indicate the geo-model is

8   geologically consistent. However, if the event timeline is manipulated to generate inconsistencies without altering

9   spatial relations (Figure 11), then an intersection between the third deposited layer (blue) and the first fault (red) is

10   detected, which is inconsistent with the altered event history (Figure 12).

11
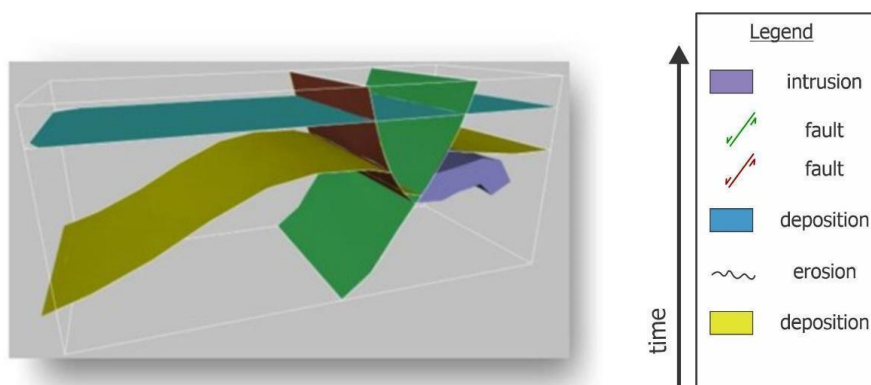
12

13   **Figure 9.** Synthetic geo-model for the GOCAD/SKUA case study: two sedimentary horizons (in yellow and blue),
14   one intrusion (in purple), two faults (in green and red), one fold (in the yellow horizon) and one erosion
15   surface (top of the yellow unit). Horizons define the top of a unit. For simplicity we ignore the folding event
16   that affects pre-erosion sediments.
17

Name	Entity type	Age	Polarity
Intrusion_A	Intrusion Unit	Youngest	Up
Fault_2	Fault Surface	Younger than F1	None
Fault_1	Fault Surface	Older than F2 Younger than HB	None
Horizon_B	Depositional Unit	Younger than HAE	Up
Horizon_A_Erosion	Erosional Surface	Younger than HA	Up
Horizon_A	Depositional Unit	Oldest	Up

1

2   **Table 4.** Local knowledge list for the GOCAD/SKUA case study.
3
4
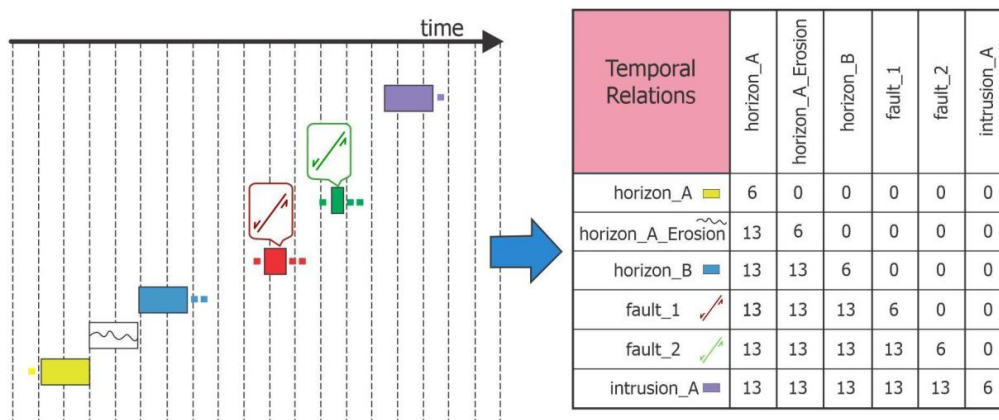
5

6   **Figure 10.** Event history (left) and temporal matrix (right) for the GOCAD/SKUA case study. For temporal relation
7   codes see Figure 6.

Spatial Relations	horizon_A	horizon_A_Erosion	horizon_B	fault_1	fault_2	intrusion_A
horizon_A	8	1	1	2	2	1
horizon_A_Erosion	1	8	0	2	2	0
horizon_B	1	0	8	2	2	0
fault_1	2	2	2	8	1	0
fault_2	2	2	2	1	8	1
intrusion_A	1	0	0	0	1	8

1

2 **Table 5.** Spatial relation matrix for the GOCAD/SKUA case study. For spatial relation codes see Figure 7.

Temporal Relations	horizon_A	horizon_A_Erosion	horizon_B	fault_1	fault_2	intrusion_A
horizon_A	6	0	0	0	0	0
horizon_A_Erosion	13	6	0	13	0	0
horizon_B	13	13	6	13	0	0
fault_1	13	0	0	6	0	0
fault_2	13	13	13	13	6	0
intrusion_A	13	13	13	13	13	6
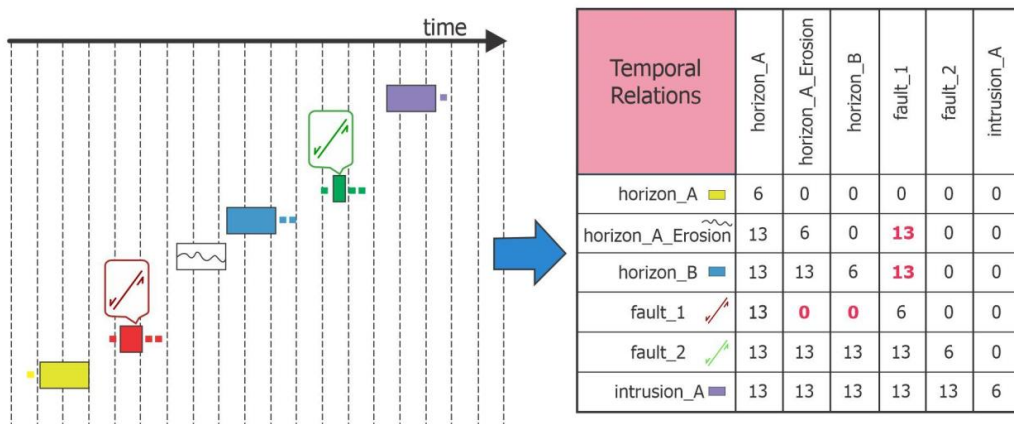
3
4

1 **Figure 11.** Modified event history (left) and temporal matrix (right) for the GOCAD/SKUA case study, with
2   unfeasible temporal relations (in red). For temporal relations codes see Figure 6.

3
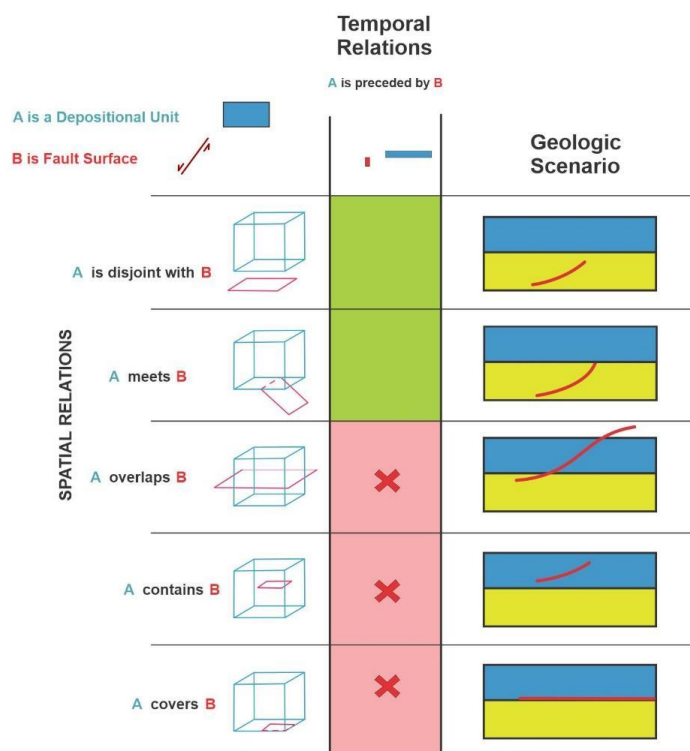
4

5 **Figure 12**. Truth table fragment indicates the relation between fault_1 (earliest fault in red) and Unit B (Blue) is not
6   consistent with the altered history. The inconsistent conditions (marked 'X') in this case are: A *overlaps* B, A
7   *contains* B, and A *covers* B, which are all geologically not plausible given the early fault is eroded BEFORE
8   deposition of UNIT B for the altered history. The acceptable consistent scenarios, in green, that are allowed
9   are possible because of the temporal A *is preceeded by* B relation since there is a time gap to allow the fault to
10   be preserved in the underlying host rock either with a hiatus in movement of the fault, or an intervening
11   erosional event introduced with the change in the event history. In all other scenarios Unit B (blue) does not
12   yet exist to host the fault.
13

14

15

16

1 **4.3 Western Canada Case Study**

2 The geo-model for this real case study (Figure 13) uses data from the Rocky Mountains of the Western Canadian

3 Cordillera, and is built using the GOCAD/SKUA, SURFE, and SPARSE toolkits (Dutranois, et al. 2010, Hillier et

4 al. 2014, de Kemp et al. 2016). It represents a portion of an east verging fold and thrust belt that has telescoped the

5 Paleozoic and basement meta-sediments of the early North American craton margin, with tectonic deformation

6 having produced in-sequence and out-of-sequence thrusts (McMechan et al., 2021, Morely 1988), as well as later

7 normal faults, with fold-fault and horizon relations that complicate original stratigraphy. The event history (Figure

8 14) is simplified with all the sedimentary units depositing sequentially, and incurring some facies changes across

9 major structures, followed by several episodes of faulting with some overlapping in time. The spatial complexity of

10 the model arises from the multitude of entities, from faults crosscutting other faults and impacting the pre-deposited

11 layers. The resulting geometry is composed of 213 objects within the 25 units, and 6 faults, with each object

12 delimited or separated from the rest of the unit by a fault.

13

14

15
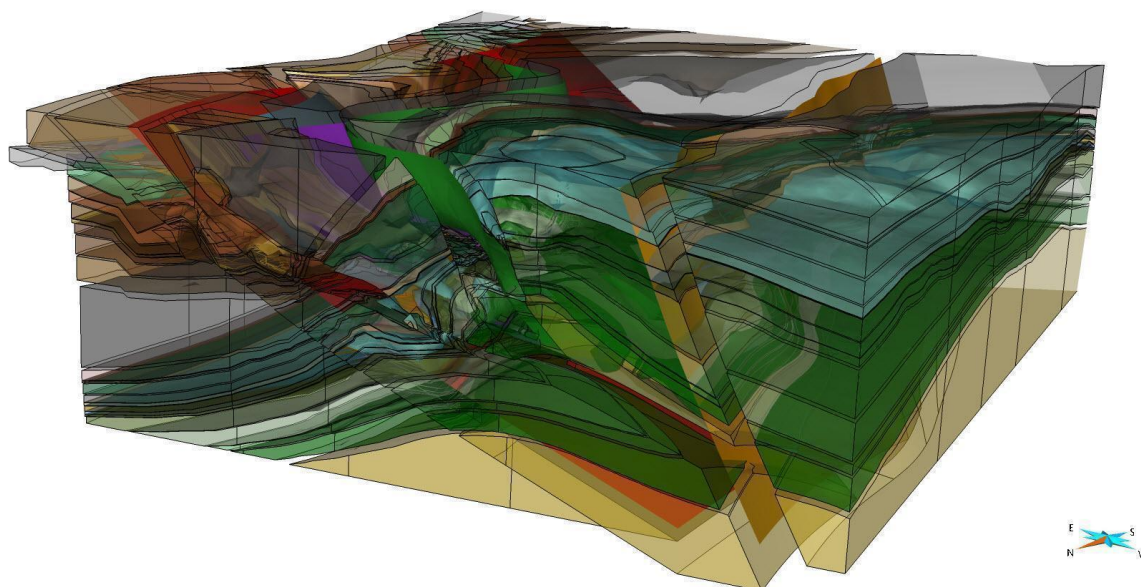
16
17

18 **Figure 13**. Western Canada case study geo-model: 213 component objects of 25 geological depositional units, and 6
19 faults.

20
21
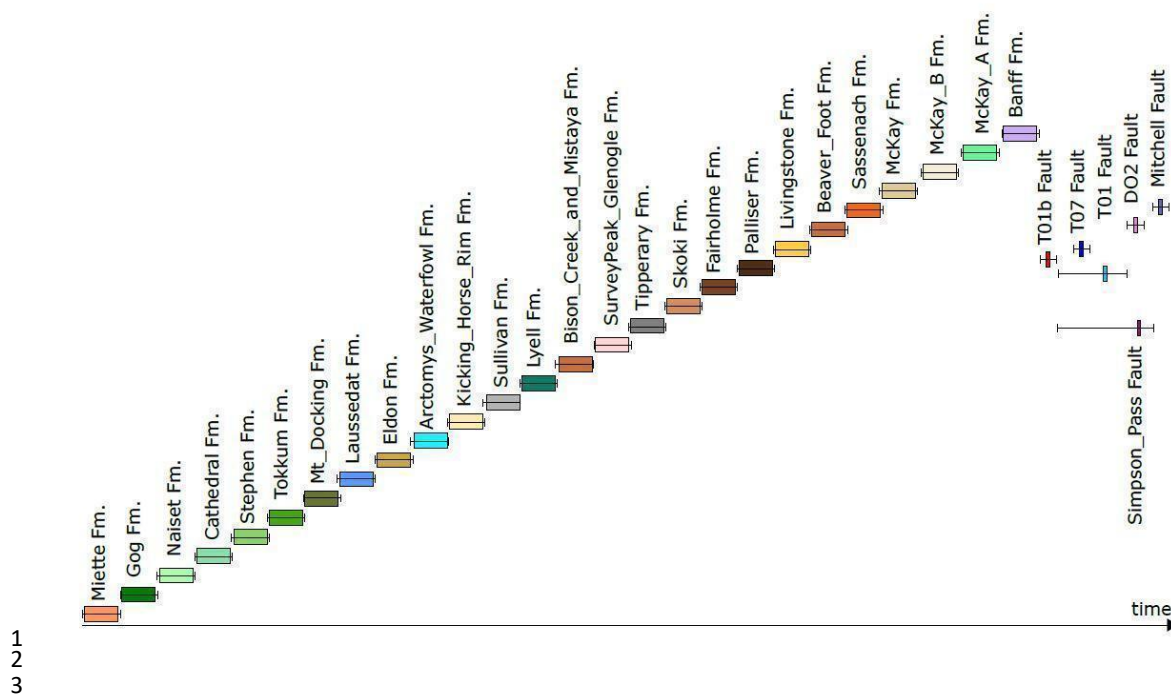
Figure 14. Event history for the Western Canada case study: horizontal boxes are relative timelines and bars are possible ranges.

After compilation of the local knowledge list and temporal relation matrix from external sources, including maps and reports, and development of the spatial relation matrix (Table 6), the consistency checker detects one inconsistency. The inconsistency (Figure 15) involves the spatial containment of one sedimentary unit (Miette) by another (Gog), which is impossible given they cannot occupy the same space, being caused by different depositional processes at different times. The consistency checker not only identifies the kind of inconsistency, through specification of the truth table cell, but it also pinpoints the location of the problem by identifying the inconsistent volumes, after iteration through all the geo-object pairs. Subsequent analysis of the inconsistency suggests it is an artifact of the modelling algorithm and its inaccurate interpolation of the data.

| Spatial Relations	Miette	Gog	Naiset	Cathedral	Tokkumm	Mt_Docking	Laussedat	Eldon	Arctomys_Waterfowl	Kicking_Horse_Rim	Sullivan	Lyell	Bison_Creek_and_Mistaya	SurveyPeak_Glenogle	Tipperary	Skoki	Fairholme	Palliser	Livingstone	Beaver_Foot	Sassenach	McKay	McKay_A	Banff	Kana_Topography	T01b_fault	T07_fault	T01_fault	Simpson Pass_fault	D02_fault	Mitchell_fault
Miette	8	5	1	1	1	1	1	1	1	1	1	1	1	1	1	0	0	0	0	0	0	0	0	0	0	2	2	0	2	2	2
Gog	4	8	1	1	1	1	1	1	1	1	1	1	1	1	1	1	1	1	1	1	1	0	0	0	0	2	2	0	2	2	2
Naiset	1	1	8	1	1	1	1	1	1	1	1	1	1	1	1	1	1	1	1	1	1	0	0	0	0	2	2	0	2	2	2
Cathedral	1	1	1	8	1	1	1	1	1	1	1	1	1	1	1	1	1	1	1	1	1	0	0	0	0	2	2	0	2	2	2
Tokkumm	1	1	1	1	8	1	1	1	1	1	1	1	1	1	1	1	1	1	1	1	1	0	0	0	0	2	2	0	2	2	2
Mt_Docking	1	1	1	1	1	8	1	1	1	1	1	1	1	1	1	1	1	1	1	1	1	0	0	0	0	2	2	0	2	2	2
Laussedat	1	1	1	1	1	1	8	1	1	1	1	1	1	1	1	1	1	1	1	1	1	0	0	0	0	2	2	0	2	2	2
Eldon	1	1	1	1	1	1	1	8	1	1	1	1	1	1	1	1	1	1	1	1	1	0	0	0	0	2	2	0	2	2	2
Arctomys_Waterfowl	1	1	1	1	1	1	1	1	8	1	1	1	1	1	1	1	1	1	1	1	1	0	0	0	0	2	2	0	2	2	2
Kicking_Horse_Rim	1	1	1	1	1	1	1	1	1	8	1	1	1	1	1	1	1	1	1	1	1	0	0	0	0	2	2	2	2	2	2
Sullivan	1	1	1	1	1	1	1	1	1	1	8	1	1	1	1	1	1	1	1	1	1	0	0	0	0	2	2	2	2	2	2
Lyell	1	1	1	1	1	1	1	1	1	1	1	8	1	1	1	1	1	1	1	1	1	0	1	0	0	2	2	2	2	2	2
Bison_Creek_Mistaya	1	1	1	1	1	1	1	1	1	1	1	1	8	1	1	1	1	1	1	1	1	0	1	0	1	2	2	2	2	2	2
Survey_Peak_Glenogle	1	1	1	1	1	1	1	1	1	1	1	1	1	8	1	1	1	1	1	1	1	0	1	0	1	2	2	2	2	2	2
Tipperary	1	1	1	1	1	1	1	1	1	1	1	1	1	1	8	1	1	1	1	1	1	1	1	0	1	2	2	2	2	2	2
Skoki	0	1	1	1	1	1	1	1	1	1	1	1	1	1	1	8	1	1	1	1	1	1	1	0	1	2	2	2	2	2	2
Fairholme	0	1	1	1	1	1	1	1	1	1	1	1	1	1	1	1	8	1	1	1	1	1	1	0	1	2	2	2	2	2	2
Palliser	0	1	1	1	1	1	1	1	1	1	1	1	1	1	1	1	1	8	1	1	1	1	1	0	1	2	2	2	2	2	0
Livingstone	0	1	1	1	1	1	1	1	1	1	1	1	1	1	1	1	1	1	8	1	1	1	1	1	1	2	2	2	2	2	0
Beaver_Foot	0	1	1	1	1	1	1	1	1	1	1	1	1	1	1	1	1	1	1	8	1	1	1	1	1	2	2	2	2	2	0
Sassenach	0	1	1	1	1	1	1	1	1	1	1	1	1	1	1	1	1	1	1	1	8	1	1	1	1	2	2	2	2	2	0
McKay	0	0	0	0	1	0	0	0	0	0	1	1	1	1	1	1	1	1	1	1	1	8	1	1	1	2	2	2	2	2	0
McKay_A	0	0	0	0	0	0	0	0	0	0	0	0	0	0	0	1	1	1	1	1	1	1	8	1	1	0	2	0	1	2	0
Banff	0	0	0	0	0	0	0	0	0	0	0	1	1	1	1	1	1	1	1	1	1	1	1	8	1	2	2	2	2	2	0
Kana_Topography	0	0	0	0	0	0	0	0	0	0	0	0	0	0	0	0	1	1	1	1	1	1	1	1	8	0	0	2	0	0	0
T01b_fault	2	2	2	2	2	2	2	2	2	2	2	2	2	2	2	2	2	2	2	2	2	0	2	0	0	8	0	0	1	0	0
T07_fault	2	2	2	2	2	2	2	2	2	2	2	2	2	2	2	2	2	2	2	2	2	2	2	0	0	0	8	0	1	1	1
T01_fault	0	0	0	0	0	0	0	0	0	2	2	2	2	2	2	2	2	2	2	2	2	2	2	2	2	0	0	8	0	1	0
Simpson Pass_fault	2	2	2	2	2	2	2	2	2	2	2	2	2	2	2	2	2	2	2	2	2	2	2	2	0	1	1	0	8	0	1
D02_fault	2	2	2	2	2	2	2	2	2	2	2	2	2	2	2	2	2	2	2	2	2	2	2	2	0	1	1	1	0	8	1
Mitchell_fault	2	2	2	2	2	2	2	2	2	2	2	2	2	2	2	2	2	0	0	0	0	0	0	0	0	0	1	0	1	1	8

Spatial Relations Legend:

0 = disjoint	3 = overlaps, is overlapped by	6 = covers
1 = meets, is met by	4 = contains	7 = is covered by
2 = intersects	5 = is contained by	8 = equals

Table 6. Spatial relation matrix for the Western Canada case study, with the inconsistent containment relations in red.
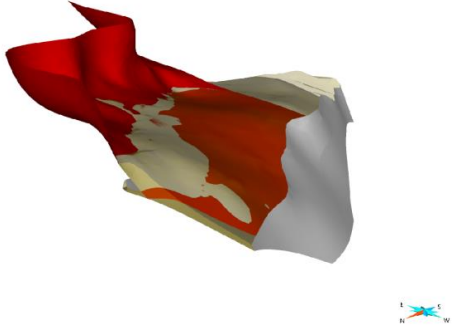
Figure 15. Inconsistent spatial containment between the Gog (red) and Miette (yellow) units in the Western Canada case study. The Miette is an older unit preceding deposition of Gog material and should not, at this scale, have a 'Miette contains Gog' spatial relation.

4.4 Noddy Case Study

The synthetic geo-model for this case study is generated using Noddy, which is a 3D rule-based modelling tool

(Jessell, 1981) that applies an input list of geological events, or event schema (Perrin et al. 2013), to a volume of

interest from which a spatial topology can be generated between objects in the volume. The event history for this

case study is quite simple, including 5 major events, deposition, tilting, folding, faulting, and intrusion (Figure 16),

from which the local knowledge list and temporal matrix are derived. The resulting geo-model (Figure 17) has an

initial depositional sequence involving 6 depositional units (represented by their top horizons), an early tilting event

followed by folding and normal faulting, and an intrusive body subsequently injected into all previous geological

objects, with the fault cutting all the horizons but not the intrusion body. Navigation of the BREP representation of

the geo-model yields a rich temporal matrix (Table 7) and spatial matrix (Table 8a).
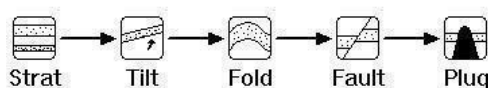
Figure 16. Event history for the Noddy case study: the Stratigraphic event is the deposition of 6 geological units in
sequence.
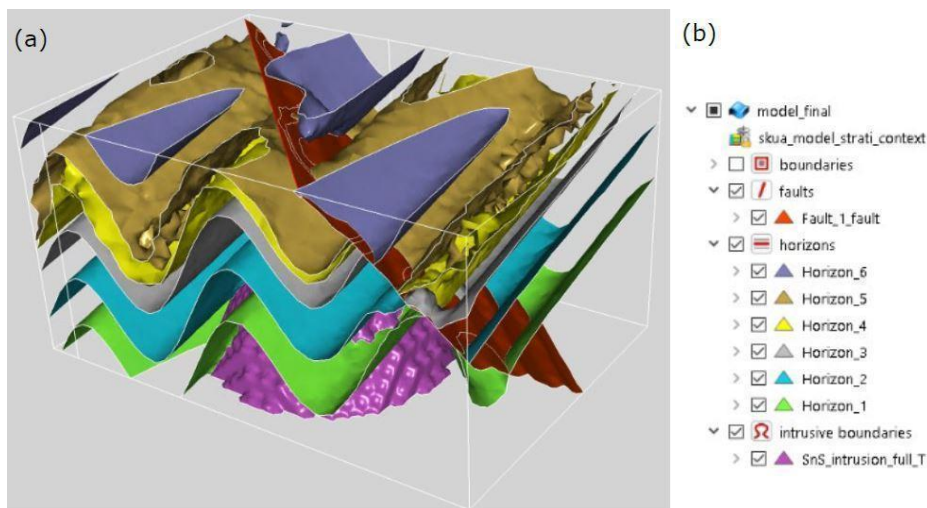
Figure 17. 3D geo-model for the Noddy case study.

TIME	Horizon_1	Horizon_2	Horizon_3	Horizon_4	Horizon_5	Horizon_6	Above Horizon 6	Fault	Intrusion
Horizon_1	6	0	0	0	0	0	0	0	0
Horizon_2	13	6	0	0	0	0	0	0	0
Horizon_3	13	13	6	0	0	0	0	0	0
Horizon_4	13	13	13	6	0	0	0	0	0
Horizon_5	13	13	13	13	6	0	0	0	0
Horizon_6	13	13	13	13	13	6	0	0	0
Above Horizon 6	13	13	13	13	13	13	6	0	0
Fault	13	13	13	13	13	13	13	6	0
Intrusion	13	13	13	13	13	13	13	13	6

1

2 **Table 7.** Temporal relations matrix for the Noddy case study. Temporal codes used here; 0 = precedes, 6 = equals,
3   13 = preceded by.

4
5

6 As an unconstrained (knowledge based) geo-modelling tool, Noddy will always produce a consistent model.

7 However, export to GOCAD/SKUA via the DXF file format results in a different spatial relation matrix, as several

8 geologically consistent but nevertheless suspect spatial relations are introduced. First, every unit spatially *meets* (i.e.

9 touches) every other unit (Table 8b), which although not impossible is somewhat suspicious, given it contradicts the

10 original Noddy model. As the resolution of the Noddy model is quite low, it seems likely that unit volume mesh

11 extents might have been mis-calculated during export to GOCAD/SKUA, to cause the dubious relations. Although

12 the relations between pairs of objects are individually consistent in this model, it is unlikely that ALL unit pairs

13 display a *meets* relation.

14

a)

SPACE	Horizon_1	Horizon_2	Horizon_3	Horizon_4	Horizon_5	Horizon_6	Above Horizon 6	Fault	Intrusion
Horizon_1	8	1	0	0	0	0	0	2	2
Horizon_2	1	8	1	0	0	0	0	2	2
Horizon_3	0	1	8	1	0	0	0	2	2
Horizon_4	0	0	1	8	1	0	0	2	2
Horizon_5	0	0	0	1	8	1	0	2	2
Horizon_6	0	0	0	0	1	8	1	2	2
Above Horizon 6	0	0	0	0	0	1	8	2	2
Fault	2	2	2	2	2	2	2	8	0
Intrusion	2	2	2	2	2	2	2	0	8

b)

SPACE	Horizon_1	Horizon_2	Horizon_3	Horizon_4	Horizon_5	Horizon_6	Above Horizon 6	Fault	Intrusion
Horizon_1	8	1	**1**	**1**	**1**	**1**	**1**	2	2
Horizon_2	1	8	1	**1**	**1**	**1**	**1**	2	2
Horizon_3	**1**	1	8	1	**1**	**1**	**1**	2	2
Horizon_4	**1**	**1**	1	8	1	**1**	**1**	2	2
Horizon_5	**1**	**1**	**1**	1	8	1	**1**	2	2
Horizon_6	**1**	**1**	**1**	**1**	1	8	1	2	2
Above Horizon 6	**1**	**1**	**1**	**1**	**1**	1	8	2	2
Fault	2	2	2	2	2	2	2	8	0
Intrusion	2	2	2	2	2	2	2	0	8

1

Table 8. Spatial relations matrix for Noddy case study, including (a) original model, and (b) after export via DXF to GOCAD/SKUA. Note the replacement of many *is disjoint with* relations (**0**) in (a), with *meets / is met by* (**1**) in (b).

5 Discussion

The consistency-checking framework and tool presented in this article are a first step toward the automated assessment of geological consistency in 3D geological models. The approach yields promising results in the four case studies: given minimal knowledge typically accompanying a 3D model, it detects geological inconsistencies that contravene geological principles as captured in the Truth Tables. However, there is much room for improvement in assessing the consistency of complex situations: the checker assesses the validity of a single geological relation in isolation, but as evident from the Noddy case study (Table 8b), a collection of relations can be inconsistent even if each relation is consistent. Assessing such relation combinations remains a future task.

To help differentiate equiprobable models, another future consideration is the development of consistency metrics for quantitative assessment of the overall quality of a 3D geo-model. These might include a cumulative consistency score to gauge the overall effect of inconsistencies on the model, as well as perhaps targeted consistency scores for specific geological relations. The latter would be particularly useful to differentiate (1) models with few inconsistencies but deep impact on internal model architecture, from (2) models with many inconsistencies but low impact on internal architecture.

Several aspects of the consistency-checking workflow could be improved:

- API: development of a simple API (Application Programming Interface) to the Truth Tables, to enable consistency-checking from a variety of software environments, including possibly those with streamlined spatial navigation mechanisms not necessarily requiring conversion to BREP.
- Enhanced Output: from the current application or prospective API, to enhance both formatting and content, such as encoding conflicting objects using knowledge graphs or spatial standards to improve visualization and understanding.
- Polarity: more automated tools could be incorporated to determine summary internal polarity for an object, and polarity relations between objects. The internal polarity of an object is rarely available in local knowledge, though potentially can be calculated from the modelling algorithm, e.g. as part of the scalar field gradient direction in implicit modelling. Supplementation from added methods also would be beneficial, e.g. from: point observations at the top horizon of a depositional unit; paleo-traces inside the unit in the case of eroded tops; the

1   cooling surface of an intrusion or extrusion; the regional or contact metamorphic gradient for a metamorphic

2   unit; or fold vergence and principal strain gradients (Fossen, 2016; Alsop, 1999; Finkl, 1984). A further

3   refinement might use local internal polarity vectors to determine polarity relations, rather than summary vectors.

4   ● Spatial relations: in a robust solution, spatial relations would be evaluated between the fragments of geological

5   objects, not between their wholes, with consistency-checking then occurring over the fragments. It also might

6   be a worthwhile experiment to include lower-dimensional representations as relata in the spatial relations, e.g.

7   allowing surfaces to represent volumetric units.

8   ● Expanding the range of model inputs to include 2D maps, cross-sections and drill logs. These representations

9   could also be checked with the same approach to see if all representations of a model are collectively consistent.

10   Consistency-checking also could be improved conceptually by: expanding the list of geological objects to include

11   fault types (e.g. normal, reverse, strike slip); expanding the associated knowledge to include fault domains (e.g.

12   upper-crust/thin-skin, deep-crust/ductile); or adding kinematic directions as additional parameters in the Truth

13   Tables, thus expanding the framework space. This would enable, for example, comparison of macro properties such

14   as nature of the deformation system with the observed local kinematic conditions, e.g. thrusting or normal fault

15   displacements.

16

17   As most 3D modeling algorithms and tools typically do not generate solid volumes in which one is fully contained

18   or covered by the other, we have set these relations as invalid for this work, knowing their presence likely indicates

19   a modeling problem and hence an inconsistency. However, as algorithms will no doubt mature, future work should

20   amend the truth tables to reflect the potential validity of such cases. This might include further extended parameters,

21   such as for parthood to indicate if a geological object is validly part of another, e.g. a formation part of a group.

22

23   More generally, broadening the underlying notion of reasonableness, which thus far is roughly equated with

24   consistency, would yield further theoretical gains. An important assumption in the existing approach is the

25   correctness of input geological knowledge. As such knowledge typically reflects the understanding of domain

26   experts, inconsistent models often differ from the expectations of these experts (van Giffen et al., 2022; McKay and

27   Harris, 2016; Burch, 2003). However, the correctness of input knowledge is a dangerous assumption, as it is more

28   likely that input knowledge is incomplete and has gaps, biasing expert expectations. It is necessary then to broaden

29   notions of geological reasonableness beyond the binary categories of consistent and inconsistent. Indeed, if we

1   consider input knowledge might be grossly good (e.g. true) or bad (e.g. false), and models consistent or inconsistent

2   with input knowledge, then four kinds of reasonableness emerge, as per Table 9: reasonable, unreasonable,

3   reasonably bad, and unreasonably bad. Reasonable models, generally preferred, are consistent with good input

4   knowledge and data constraints. Unreasonable models have geological relations inconsistent with good input

5   knowledge. Reasonably bad models have geological relations that fit with the input knowledge, but this knowledge

6   is wrong, or incomplete, so the model is variously questionable. Unreasonably bad models have input knowledge

7   that may be wrong, and the model is also inconsistent, because of algorithm bias, scale/resolution, constraint data

8   configuration or other processing errors. Inconsistent models thus signal a need to adjust the algorithm or investigate

9   the input data and knowledge. Note, however, all models might be useful (Gleeson et al, 2021), as any geo-model

10   from bad knowledge might be preferred to no models, or models with no input knowledge; and an inconsistent

11   model from good knowledge, that is unreasonable, might be preferable to the alternatives, especially in parts where

12   it is actually consistent.

13

14

Model Consistency

	Inconsistent	**Consistent**
Good Knowledge	Unreasonable	Reasonable
Bad Knowledge	Unreasonably Bad	Reasonably Bad

15

16

17   **Table 9**. Types of 3D geo-model consistency.
18

19   It is also noteworthy, and sobering, that an ideal model could arise from any of the four categories, simply because

20   the combination of input knowledge, data, and computational processes just happens to produce the best result.

21   Consistency-checking thus provides only some insight as to whether an ideal model is achieved, as one would hope

22   an ideal model should be consistent more often than not. For example this should be the case when comparing a

23   suite of models and their flow characteristics, with 'reasonable' models matching the real world historical

1 production curves (Melnikova et al., 2012). Mounting evidence suggests even a minimum of geological knowledge

2 and improved consistency with this knowledge can improve the utility of models (Giraud et al., 2020).

3

4 Finally, application of the framework to case studies at various scales, using different tools and algorithms, would

5 provide further insight into its utility for: exploring different levels of geological and model complexity (Pellerin et

6 al., 2015); comparing high-resolution to generalized regional models; testing more speculative models; for

7 correlation of jurisdictional bordered models (e.g. comparing number and variety of entities, and consistency with

8 each other) and finally for assessing the range of equiprobable 3D geological models created from probabilistic and

9 future generative AI methods.

10

11 **6 Summary**

12 Due to the increasing complexity of current geo-modelling algorithms, leading to a plethora of models of variable

13 quality, there is a clear need for an approach to check the geological consistency of a model. To this end, the

14 consistency checker framework and proof-of-concept tool successfully verify geo-models in four case studies,

15 confirming consistencies and finding inconsistencies. Inputs include knowledge typically available with any

16 geological model, namely, the spatial-temporal-polarity relations between pairs of geological objects. A specific

17 combination of these inputs serves as an index into a Truth Table documenting a possible geological situation that is

18 either consistent or inconsistent with established geological principles. As the situations in the framework are quite

19 general, there is significant potential to expand the space with additional parameters, such as tectonic or parthood.

20 To better determine effectiveness, further testing also is required on large numbers of models representing a variety

21 of geological situations, at different scales, with models made using diverse tools and algorithms. Altogether, this

22 work represents a first step toward the real-time consistency-checking of geo-models; therefore, it also has the

23 potential to inform consistency-checking during model-building, to help increase knowledge constraints in geo-

24 modelling algorithms.

25
26
27
28
29
30
31
32
33
34
35

1
2
3
4
5
6
7
8
9
10
11 **Appendix**
12
13 **Algorithm 1: Consistency-checking**
14
15 **Require:** *Mspatial* spatial relationship matrix, *Mtemporal* temporal relationship matrix, *LNaturePolarity* nature and
16 polarity matrix of entities, *Truthtable* 'Truth Tables' for each pair of geological entities, *LGeologicalEntities* list
17 of all geological entities detected in the 3D model.
18 **Initialize (empty):** *Linconsistencies* list of inconsistencies detected inside the given 3D geological model
19   **for** each *GeolEntity* in *LGeologicalEntities* **do**
20   **for** each *GeolEntity* in the remaining rows in *LGeologicalEntities* **do**
21   extract the name, nature and polarity in each geological entity from *LNaturePolarity*
22   given both geological entities, find the corresponding truth table *Truthtable*
23   deduce the polarity relation from both geological entities: aligned, opposed, unknown
24   extract the spatial relationship for the pair of geological entities from *Mspatial*
25   transform the spatial relationship into a row in the truth table
26   extract the temporal relationship for the pair of geological entities from *Mtemporal*
27   transform the temporal relationship into a column in the truth table
28   **if** the statement found in the corresponding truth table is 'inconsistent' **then**
29   **for** each part in each *GeolEntity* **do**
30   **for** each part in each *GeolEntity* **do**
31   extract the name, nature and polarity of each geological entity inside *LNaturePolarity*
32   given both geological entities, find the corresponding truth table *Truthtable*
33   deduce the polarity relation from both geological entities: aligned, opposed, unknown
34   extract the spatial relationship for the pair of geological entities from *Mspatial*
35   transform the spatial relationship into a row in the truth table
36   extract the temporal relationship for the pair of geological entities from *Mtemporal*
37   transform the temporal relationship into a column in the truth table
38   **if** the statement found in the corresponding truth table is 'inconsistent' **then**
39   **for** each part in each part of *GeolEntity* **do**
40   **for** each part in each part of *GeolEntity* **do**
41   etc...
42   **end for**
43   **end for**
44   **end if**
45   **end for**
46   **end for**
47   **end if**
48   add the statement found in the corresponding truth table to *Linconsistencies*
49   **end for**
50   **end for**
51   **return** *Linconsistencies*

52

53 **Code and Data Availability**

54 Consistency-inconsistency matrices called 'Truth Tables' used for determining validity of geological spatial-
55 temporal relations **https://doi.org/10.5281/zenodo.10909160**, (de Kemp, 2024).
56

1   **Video Supplement**
2   There are currently no video files (mp4) related to this article.

3   **Author contributions**
4   Conceptualization by MP, EdK, BB and MH; MP developed the tool; MP, EdK, BB and MH all contributed to the
5   case studies development and the writing of the paper.

6   **Competing interests**
7   The author declares that there is no conflict of interest.

8   **Special Issue Statement:** This contribution is part of the Loop stochastic geological modelling platform –
9   development and applications, edited by Laurent Ailleres
10   (https://gmd.copernicus.org/articles/special_issue1142.html, last access: 6 April 2024).

23   **References**

24   Allen, J. F.: Maintaining knowledge about temporal intervals, Communications of the ACM, 26, 832–843, 1983.

25   Alsop, G.I., Holdsworth, R.E.: Vergence and facing patterns in large scale sheath folds. Journal of Structural
26   Geology 21, 1335-1349, 1999.

27   Annen, C.: Implications of incremental emplacement of magma bodies for magma differentiation, thermal aureole
28   dimensions and plutonism–volcanism relationships, Tectonophysics, 500 (1-4), 3-10,
29   https://doi.org/10.1016/j.tecto.2009.04.010, 2011.

30   Arora, H.: Langenhan, C., Petzold, F., Eisenstadt, V., and Althoff, K.-D.: METIS-GAN: An approach to generate
31   spatial configurations using deep learning and semantic building models, in: ECPPM 2021–eWork and
32   eBusiness in Architecture, Engineering and Construction, pp. 535 268–273, CRC Press, 2021.

33   Aubry, M.P, Berggren, W.A., Van Couvering, J.A. and Steininger,F.:Problems in chronostratigraphy: stages, series,
34   unit and boundary stratotypes, global stratotype section and point and tarnished golden spikes,Earth-Science
35   Reviews, 46, (1–4), 99-148, ISSN 0012-8252, https://doi.org/10.1016/S0012-8252(99)00008-2, 1999.

36   Bai, H., Montési, L.G.J. and Behn, M.D. :MeltMigrator: A MATLAB-basedsoftware for modeling three-
37   dimensional melt migration and crustal thickness variations at mid-ocean ridges following a rules-based
38   approach, Geochem. Geophys. Geosyst., 18, 445–456, https://doi.org/10.1002/2016GC006686, 2017.

39   Banerjee, P. K., Banerjee, P. K., and Butterfield, R.: Boundary element methods in engineering science, McGraw-
40   Hill (UK), 1981.

41   Bertoncello, A., Sun, T., Li, H. Mariethoz, G. and Caers, J.: Conditioning Surface-Based Geological Models to Well
42   and Thickness Data. Math. Geosci., 45, 873–893 (2013). https://doi.org/10.1007/s11004-013-9455-4, 2013.

1   Bezhanishvili, N., Ciancia, V., Gabelaia, D., Grilletti, G., Latella, D. and Massink, M.: Geometric Model Checking
2   of Continuous Space, Logical Methods in Computer Science Volume 18, Issue 4, 2022, pp. 7:1–7:38,
3   https://doi.org/10.46298/lmcs-18(4:7)2022.

4   Bond, C.E.: Uncertainty in structural interpretation: Lessons to be learnt, Jour. Struct. Geol., 74, 185-200, ISSN
5   0191-8141, https://doi.org/10.1016/j.jsg.2015.03.003, 2015.

6   Botella, A., Lévy, B. and Caumon, G.: Indirect unstructured hex-dominant mesh generation using tetrahedra
7   recombination, Comp. Geosci., 20, 437–451, https://doi.org/10.1007/s10596-015-9484-9, 2016.

8   Brodaric, B.: Characterizing and representing inference histories in geologic mapping, Int. Jour. Geog. Info. Sci., 26
9   (2), 265-281, https://doi.org/10.1080/13658816.2011.585992, 2012.

10 Brodaric, B. and Gahegan, M.: Representing Geoscientific Knowledge in Cyberinfrastructure: challenges,
11   approaches and implementations. In: Sinha, A.K. (Ed.), Geoinformatics, Data to Knowledge, Geological
12   Society of America Special Paper 397, pp. 1-20. https://doi.org/10.1130/2006.2397(01), 2006.

13 Brodaric, B., Gahegan, M., Harrap, R.: The art and science of mapping: Computing geological categories from field
14   data, Comp. Geos., 30 (7),719-740, https://doi.org/10.1016/j.cageo.2004.05.001, 2004.

15 Burch, T.K.: Data, Models, Theory and Reality: The Structure of Demographic Knowledge. In: Billari, F.C.,
16   Prskawetz, A. (eds) Agent-Based Computational Demography. Contributions to Economics. Physica,
17   Heidelberg, https://doi.org/10.1007/978-3-7908-2715-6_2 , 2003.

18 Burns, K.L.: Analysis of geological events, Mathematical Geology, 7, 295–321, 1975.

19 Burns, K.L., Shepherd, J. and Marshall, B.: Analysis of Relational Data from Metamorphic Tectonites: Derivation of
20   Deformation Sequences from Overprinting Relations, Proceedings of the International Association for
21   Mathematical Geology (IAMG) 25th International Congress in Sydney, Australia, August 1976, In: Recent
22   Advances in Geomathematics, An International Symposium, Edited by D.F. Merriam, Syracuse University,
23   Computers and Geology Volume 2, 171-199, 1978.

24 Burns, K.L. and Remfry, J.G., 1976, A Computer Method of Constructing Geological Histories from Field Surveys
25   and Maps, Computers and Geosciences, Vol. 2, 141-162, 1976.

26 Burns, K.L., Marshall, B. and Gee, R.D.: Computer-Assisted Geological Mapping, Proceedings of the Australian
27   Institute of Mining and Metallurgy, 323, 41-47, 1969.

28 Cherpeau, N., Caumon, G., and Lévy, B.: Stochastic simulations of fault networks in 3-D structural modelling:
29   Comptes Rendus Geosciences, 342, 687−694, 2010.

30 Claramunt, C. and Jiang, B.: An integrated representation of spatial and temporal relationships between evolving
31   regions, Journal of geographical systems, 3, 411–428, 2001.

32 Crossley, M. D.: Essential topology, Springer-Verlag, London, 226 pp, ISBN 1-85233-782-6, 226, 2005.

33 de la Varga, M., Schaaf, A., and Wellmann, F.: GemPy 1.0: opensource stochastic geological modeling and
34   inversion, Geosci. Model Dev., 12, 1–32, https://doi.org/10.5194/gmd-12-1-2019, 2019.

35 de la Varga, M., Wellmann, J.F.: Structural geologic modeling as an inference problem: A Bayesian perspective,
36   Interpretation, 4(3), pp. SM15-SM30, http://dx.doi.org/10.1190/INT-2015-0188.1, 2016.

37 de Kemp, E.A.: Truth Tables for consistency-checking 3D geological models, Zenodo,
38   https://doi.org/10.5281/zenodo.10909160, 2024.

39 de Kemp, E. A., Jessell, M. W., Aillères, L., Schetselaar, E. M., Hillier, M., Lindsay, M. D., and Brodaric, B.: Earth
40   model construction in challenging geologic terrain: Designing workflows and algorithms that makes sense, in:
41   Proceedings of Exploration'17: Sixth DMEC – Decennial International Conference on Mineral Exploration,

edited by: Tschirhart, V. and Thomas, M. D., Integrating the Geosciences: The Challenge of Discovery, Toronto, Canada, 21–25 October 2017, 419–439, 2017.

de Kemp, E.A., Schetselaar, E.M., Hillier, M.J., Lydon, J.W. and Ransom, P.W.: Assessing the Workflow for Regional Scale 3D Geological Modelling: An Example from the Sullivan Time Horizon, Purcell Anticlinorium East Kootenay Region, Southeastern British Columbia, *Interpretation,* Special section: Building complex and realistic geologic models from sparse data, 4(3), p. SM33-SM50, 2016.

de Kemp, E. A., Sprague, K., and Wong, W.: Interpretive Geology with Structural Constraints: An introduction to the SPARSE © plug-in, Americas GOCAD User Meeting, Houston Texas, 1–16, https://doi.org/10.5281/zenodo.4646210, 1 November 2004.

Deutsch, C.V.: All Realizations All the Time, In: Daya Sagar, B., Cheng, Q., Agterberg, F. (eds) Handbook of Mathematical Geosciences. Springer, Cham. https://doi.org/10.1007/978-3-319-78999-6_7, 2018.

Dutranois, A., Wan-Chiu, L., Dulac, J-C, Lecomte, J-F, Callot, J-P and Rudkiewicz, J-L: Breakthrough in basin modeling using time/space frame, *OFFSHORE*, Sept. 1, 2010.

Egenhofer, M.J.: A formal definition of binary topological relationships, In: Litwin, W., Schek, HJ. (eds) Foundations of Data Organization and Algorithms, FODO 1989, Lecture Notes in Computer Science, Springer, Berlin, Heidelberg, 367, https://doi.org/10.1007/3-540-51295-0_148, 1989.

Egenhofer, M., Sharma J. and Mark D.: A critical comparison of the 4-intersection and 9- intersection models for spatial relations: formal analysis, In: R. McMaster and M. Armstrong (eds), Autocarto 11, Minneapolis, MN, 1-11, 1993.

Egenhofer, M. and Franzosa, R., 1991. Point-set topological relations. International Journal of Geographical Information Systems 5 (2): 161-174.

Fattah, M.: Physical Geology, On line course, UDEMY, (https://www.udemy.com/course/geology-fundamentalz/, last access: 6 April 2024), 2022.

Finkl C.W.:Field Geology. In: Finkl C. (eds) Applied Geology. Encyclopedia of Earth Sciences Series, vol 3. Springer, Boston, MA. https://doi.org/10.1007/0-387-30842-3_21, 1984.

Fossen H.:Structural Geology. Cambridge University Press, New York, 524, 2016.

Frodeman, R.:Geological reasoning: geology as an interpretive and historical science, Geol. Soc. Am. Bull. 107, 960e968, 1995.

Galton, A.: Spatial and temporal knowledge representation, Earth Science Informatics, pp. 169–187, https://doi.org/10.1007/s12145-0090027-6, 2009.

Geodes-Solutions, https://geode-solutions.com/opengeode/, last access: 6 April 2024).

Giraud, J., Caumon, G., Grose, L., Ogarko, V., and Cupillard, P.: Integration of automatic implicit geological modelling in deterministic geophysical inversion, Solid Earth, 15, 63–89, https://doi.org/10.5194/se-15-63-2024, 2024.

Giraud, J., Lindsay, M., Jessell, M., and Ogarko, V.: Towards plausible lithological classification from geophysical inversion: honouring geological principles in subsurface imaging, Solid Earth, 11, 419–436, https://doi.org/10.5194/se-11-419-2020, 2020.

Grose, L., Ailleres, L., Laurent, G., Armit, R., and Jessell, M.: Inversion of geological knowledge for fold geometry, J. Struct. Geol., 119, 1–14, https://doi.org/10.1016/j.jsg.2018.11.010, 2019.

Gleeson, T., Wagener, T., Döll, P., Zipper, S. C., West, C., Wada, Y., Taylor, R., Scanlon, B., Rosolem, R., Rahman, S., Oshinlaja, N., Maxwell, R., Lo, M.-H., Kim, H., Hill, M., Hartmann, A., Fogg, G., Famiglietti, J.

S., Ducharne, A., de Graaf, I., Cuthbert, M., Condon, L., Bresciani, E., and Bierkens, M. F. P.: GMD perspective: The quest to improve the evaluation of groundwater representation in continental- to global-scale models, Geosci. Model Dev., 14, 7545–7571, https://doi.org/10.5194/gmd-14-7545-2021, 2021.

Gong, P. and Mu, L.: Error detection through consistency checking, Geographic Information Sciences, 6, 188–193, 2000.

Groshong, R. H. Jr.: 3-D Structural Geology a Practical Guide to Quantitative Surface and Subsurface Map Interpretation, (2nd Edition), Springer-Verlag Berlin Heidelberg., ISBN-13, 978-3540310549, 2006.

Harrap, R.: A Legend Language for Geologic Maps, Precambrian Times, Geological Association of Canada, Precambrian Division Newsletter, Volume 01, Issue 1, Jan./Feb. 2001, p.1, 3-9, 2001.

Hillier, M. J., Wellmann, F., Brodaric, B., de Kemp, E. A., and Schetselaar, E.: Three-Dimensional Structural Geological Modeling Using Graph Neural Networks, Mathematical Geosciences, https://doi.org/10.1007/s11004-021-09945-x, 2021.

Hillier, M. J., Schetselaar, E. M., de Kemp, E. A., and Perron, G.: Three-dimensional modelling of geological surfaces using generalized interpolation with radial basis functions, Mathematical Geosciences, 46, 931–953, 2014.

Hillier, M.J., Schetselaar, E. M., de Kemp, E. A.: SURFE implicit code library repository, (Open Source), https://github.com/MichaelHillier/surfe, (last access: 6 April 2024), 2021.

Hinojosa, J.H. and Mickus, K.L.: Foreland basin-a FORTRAN program to model the formation of foreland basins resulting from the flexural deflection of the lithosphere caused by a time-varying distributed load, Comp. Geosci., 19(9), 1321-1332, https://doi.org/10.1016/0098-3004(93)90032-Z, 1993.

Hobbs, B., Regenauer-Lieb, K. and Ord, A.:Thermodynamics of Folding in the Middle to Lower Crust, Geology, 35 (2), 175-178, https://doi.org/10.1130/G23188A.1, 2007.

Jayr, S., Gringarten, E., Tertois, A.-L., Mallet, J.-L. and Dulac, J.-C.: The need for a correct geological modelling support: The advent of the UVT-transform, First Break, 26, 73-79, https://doi.org/10.3997/1365-2397.26.10.28558, 2008.

Jessell, M. W.: Noddy: an interactive map creation package, Unpublished MSc Thesis, University of London, 1981.

Jessell, M., Ogarko, V., de Rose, Y., Lindsay, M., Joshi, R., Piechocka, A., Grose, L., de la Varga, M., Ailleres, L., and Pirot, G.: Automated geological map deconstruction for 3D model construction using map2loop 1.0 and map2model 1.0, Geosci. Model Dev., 14, 5063–5092, https://doi.org/10.5194/gmd-14-5063-2021, 2021.

Jessell, M. W., Aillères, L. and de Kemp, E. A.: Towards an Integrated Inversion of Geoscientific data: what price of Geology? Tectonophysics, 490(3-4), 294-306, 2010.

Jessell, M., Aillères, L., de Kemp, E.A., Lindsay, M., Wellmann, J., Hillier, M., Laurent, G., Carmichael, T., and Martin, R.: Next generation three-dimensional geologic modeling and inversion, Society of Economic Geologists Special Publication, 18, 261–272, 2014.

Kardel, T. and Paul Maquet, P.,: Nicolaus Steno: Biography and Original Papers of a 17th Century Scientist, 2013'th (Kindle) Edition, Springer; 2013th edition, 739, ISBN-13 978-3642250781, 2012.

Lajevardi, S. and Deutsch, C.V.: Stochastic regridding of geological models for flow simulation, Bulletin of Canadian Petroleum Geology, 63 (4): 374–392, https://doi.org/10.2113/gscpgbull.63.4.374, 2015.

Lajaunie, C., Courrioux, G., Manuel, L.:Foliation fields and 3D cartography in geology: principles of a method based on potential interpolation. Math Geol 29(4):571–584, https://doi.org/10.1007/BF02775087, 1997.

Le, H.H., Gabriel, P., Gietzel, J. and Schaeben, H.:An object-relational spatio-temporal geoscience data model, Comp. Geos., 57, 104-115, ISSN 0098-3004, https://doi.org/10.1016/j.cageo.2013.04.014, 2013.

Lindsay, M.D., Aillères, L., Jessell, M.W., de Kemp, E.A., Betts, P.G.: Locating and quantifying geological uncertainty in three-dimensional models: Analysis of the Gippsland Basin, southeastern Australia, Tectonophysics, 546-547, 10-27, https://doi.org/10.1016/j.tecto.2012.04.007, 2012.

Lyell, (Sir) C..:Principles of Geology: Or, the Modern Changes of the Earth and Its Inhabitants, Considered As Illustrative of Geology, Volume 1, (Original 1833) 2022.

Legare Street Press, ISBN-13 978-1015539976, 496, (original 1833) 2022.Mallet, J-L.: Space–Time Mathematical Framework for Sedimentary Geology. Math. Geol., 36, 1–32, https://doi.org/10.1023/B:MATG.0000016228.75495.7c, 2004.

Mallet, J-L., Jacquemin, P. and Cheimanoff, N.: GOCAD project: Geometric modeling of complex geological surfaces, in: SEG Technical Program Expanded Abstracts, 126-128, https://doi.org/10.1190/1.1889515, 1989.

McKay, G. and Harris, J.R.: Comparison of the Data-Driven Random Forests Model and a Knowledge-Driven Method for Mineral Prospectivity Mapping: A Case Study for Gold Deposits Around the Huritz Group and Nueltin Suite, Nunavut, Canada. Nat. Resour. Res., 25, 125–143. https://doi.org/10.1007/s11053-015-9274-z, 2016.

McMechan, M.E., Root, K.G., Simony, P.S. and Pattison, D.R.M.:Nailed to the craton: Stratigraphic continuity across the southeastern Canadian Cordillera with tectonic implications for ribbon continent models, Geology, 49 (1): 101–105, https://doi.org/10.1130/G48060, 2021.

Melnikova, Y., Cordua, K. S., & Mosegaard, K. (2012). History Matching: Towards Geologically Reasonable Models. Abstract from EAGE Integrated Reservoir Modelling: Are we doing it right?, Dubai, United Arab Emirates.

Michalak, J.:Topological conceptual model of geological relative time scale for geoinformation systems, Comp. Geos., 31-7, 865-876, ISSN 0098-3004, https://doi.org/10.1016/j.cageo.2005.03.001, 2005.

Morley, C.K.: Out-of-sequence thrusts, Tectonics, 7 (3), 539-561, 1988.

New South Wales (NSW), Australia, Department of Primary Industries (DPI), History of Geology, February 2007, Primefacts 563, 6, (https://digs.geoscience.nsw.gov.au/api/download/c6ae94e9dc65f614492646c269ea3731/Primefact_563_Minfact_60_History_of_geology.pdf, last access: 20 April 2022).

Nikoohemat, S., Diakité, A. A., Lehtola, V., Zlatanova, S., and Vosselman, G.: Consistency grammar for 3D indoor model checking, Transactions in GIS, pp. 189–212, https://doi.org/10.1111/tgis.12686, 2021.

Pellerin, J., Caumon, G., Julio, C., Mejia-Herrera, P., Botella, A.: Elements for measuring the complexity of 3D structural models: Connectivity and geometry, Computers & Geosciences, 76, 130-140, ISSN 0098-3004, https://doi.org/10.1016/j.cageo.2015.01.002, 2015.

Pellerin, J., Botella, A., Bonneau, F., Mazuyer, A., Chauvin, B., Lévy, B., Caumon, G.: RINGMesh: A programming library for developing mesh-based geomodeling applications, Comp. Geos.,104, 93-100, ISSN 0098-3004, https://doi.org/10.1016/j.cageo.2017.03.005, 2017.

Perrin, M., Poudret, M., Guiard, N. and Schneider, S.:Chapter 6: Geological Surface Assemblage, In: Shared Earth Modeling, Knowledge driven solutions for building and managing subsurface 3D geological models, ifp Energies Nouvelles Publications - TECHNIP, Paris, France, 115-139, 2013.

Perrin, M., Morel, O., Mastella, L., and Alexandre, L.: Geological Time Formalization: an improved formal model for describing time successions and their correlation, Earth Science Informatics, pp. 81–96, https://doi.org/10.1007/s12145-011-0080-9, 2011.

1   Pyrcz, M. J., Sech, R. P., Covault, J. A., Willis, B. J., Sylvester, Z., Sun, T., and Garner, D.: Stratigraphic rule-based
2   reservoir modeling, Bulletin of Canadian Petroleum Geology, 63, 287–303, 2015.

3   Ranalli, G.:A stochastic model for strike-slip faulting. Math. Geol., 12, 399–412,
4   https://doi.org/10.1007/BF01029423, 1980.

5   Rauch, A. Sartori, M., Rossi, E., Baland, P. and Castelltort, S.: Trace Information Extraction (TIE): A new
6   approach to extract structural information from traces in geological maps, Jour. Struct. Geol., 126, 286-300,
7   ISSN 0191-8141, https://doi.org/10.1016/j.jsg.2019.06.007, 2019.

8   Rothery, D.: Geology: A Complete Introduction, Quercus; 1st edition (Feb. 16 2016), ISBN-13, 978-1473601550,
9   384, 2016.

10 Schetselaar, E. M. and de Kemp, E. A.: Topological encoding of spatial relationships to support geological
11   modelling in a 3-D GIS environment, Int. Assoc. for Mathematical Geology XIth International Congress,
12   Université de Liège - Belgium, 2006.

13 Shokouhi, P., Kumar, V., Prathipati, S., Hosseini, S.A., Giles, C.L., and Kifer, D.: Physics-informed deep learning
14   for prediction of CO2 storage site response, Journal of Contaminant Hydrology, 241, 103835, ISSN 0169-
15   7722, https://doi.org/10.1016/j.jconhyd.2021.103835, 2021.

16 Snyder, D. B., Hillier, M. J., Kjarsgaard, B. A. K., de Kemp, E. A. & Craven, J. A.: Lithospheric architecture of the
17   Slave craton, northwest Canada, as determined from an interdisciplinary 3-D model. *Geochemistry,*
18   *Geophysics, Geosystems (G3)*, 15, 1-16. https://doi.org/10.1002/2013GC005168, 2014.

19 Thapa, P. and McMechan, M.E.: Methodology for portraying 3D structure using ArcGIS: a test case from the
20   southern Canadian Rocky Mountains, British Columbia and Alberta, Geological Survey of Canada, Open File
21   8576, 17 p, 2019.

22 Thiele, S. T., Jessel, M. W., Lindsay, M., Ogarko, V., Wellmann, J. F., and Pakyuz-Charrier, E.: The topology of
23   geology 1: Topological analysis, Jour. Struct. Geol., 91, 27-38, https://doi.org/10.1016/j.jsg.2016.08.009,
24   2016a.

25 Thiele, S.T., Jessel, M.W., Lindsay, M., Wellmann, J.F. and Pakyuz-Charrier, E.: The topology of geology 2:
26   Topological uncertainty, Jour. Struct. Geol., 91, 74-87, ISSN 0191-8141,
27   https://doi.org/10.1016/j.jsg.2016.08.010, 2016b.

28 van Giffen, B. Herhausen, D., Fahse, T.: Overcoming the pitfalls and perils of algorithms: A classification of
29   machine learning biases and mitigation methods, Journal of Business Research, 144, 93-106, ISSN 0148-2963,
30   https://doi.org/10.1016/j.jbusres.2022.01.076., 2022.

31 Van Oosterom, P.: Maintaining consistent topology including historical data in a large spatial database, 13, 327–
32   336, 1997.

33 Wellmann, F. and Caumon, G.: 3-D Structural geological models: Concepts, methods, and uncertainties, Advances
34   in Geophysics, pp. 1–121, https://doi.org/10.1016/bs.agph.2018.09.001, 2018.

35 Zhan, X., Lu, C. and Hu, G.: A Formal Representation of the Semantics of Structural Geological Models, Scientific
36   Programming, 2022, 5553774, https://doi.org/10.1155/2022/5553774, 2022.

37 Zhan, X., Liang, J., Lu, C., and Hu, G.: Semantic Description and Complete Computer Characterization of Structural
38   Geological Models, Geoscientific Model Development Discussions, 1–39, 2019.

39 Ziggelaar, A.: The age of Earth in Niels Stensen's geology, Memoir of the Geological Society of America
40   ISSN:0072-1069, 203, 135-142, 2009.

41 Zlatanova, S., Rahman, A. A., and Shi, W.: Topological models and frameworks for 3D spatial objects, Comp.
42   Geos, 30, 419–428, 2004.